Journal of Theoretical Biology 257 (2009) 27–44

Contents lists available at ScienceDirect

Journal of Theoretical Biology

journal homepage: www.elsevier.com/locate/yjtbi

Mathematical model for G-CSF administration after chemotherapy

Catherine Foley [a,*], Michael C. Mackey [b,1]

[a] Department of Mathematics and Centre for Nonlinear Dynamics, Mcgill University, 3655 Promenade Sir William Osler, Montreal, Quebec, Canada H3G 1Y6
[b] Departments of Mathematics, Physics, Physiology and Centre for Nonlinear Dynamics, Mcgill University, 3655 Promenade Sir William Osler, Montreal, Quebec, Canada H3G 1Y6

ARTICLE INFO

Article history:
Received 19 March 2008
Received in revised form
12 September 2008
Accepted 23 September 2008
Available online 1 November 2008

Keywords:
Mathematical modeling
Filgrastim
Pegfilgrastim
Alternative treatment

ABSTRACT

Granulocyte-colony stimulating factor (G-CSF) is used clinically for treating chemotherapy-induced neutropenia (low neutrophil levels). Here we present a delay differential equation model for the regulation of neutrophil production that accounts for the effects of G-CSF. Using a combination of analysis and numerical simulations, we use this model to study the effects of delaying G-CSF treatment following chemotherapy for two recombinant forms of G-CSF (filgrastim and pegfilgrastim). We also examine the consequences of varying the duration of filgrastim treatment. We found that varying the starting day or the duration of G-CSF treatment can lead to different qualitative responses in the neutrophil count. These changes can be explained by the coexistence of two stable solutions in the mathematical model.

1. Introduction

Hematopoiesis is the term that refers to the production of blood cells. This process is initiated in the bone marrow by the stem cells, which are self-renewing and which can differentiate and mature to produce all types of blood cells: the leucocytes (white blood cells or WBCs), the erythrocytes (also known as red blood cells (RBCs)) and platelets. Production of blood cells is regulated by cytokines (growth factors) via negative feedback mechanisms. Erythropoietin (EPO) regulates the production of RBCs, thrombopoietin mediates platelets production whereas granulocyte-colony stimulating factor (G-CSF) regulates granulopoiesis (production of WBCs).

Neutropenia refers to a condition in which the number of neutrophils is low.

Neutrophils usually make up 50–70% of circulating WBCs and serve as the primary defence against infections by destroying bacteria in the blood. Hence, having a reduced number of neutrophils makes the body less able to fight infection and this condition can sometimes become life-threatening. Neutropenia is said to be severe if the absolute neutrophil count (ANC) is less than 500 cells per microlitre of blood (or equivalently, 0.38×10^8 cells/kg). Severe chronic neutropenia may be present at birth (congenital neutropenia) or may occur at any stage in life (acquired neutropenia). In particular, chemotherapy often causes neutropenia since it typically attacks cells indiscriminately regardless of whether malignant or normal. In fact, neutropenia is one the most frequent side-effects of chemotherapy (Rahman et al., 1997; Vainstein et al., 2005). Administration of recombinant forms of the growth factor G-CSF has been shown to stimulate neutrophil production and is now the standard treatment for neutropenia. However, the clinical administration schedule of G-CSF is typically determined by trial and error and it is not clear if there is an optimal way of giving G-CSF after chemotherapy (Clark et al., 2005; Bennett et al., 1999).

Some clinical studies have tried to optimize G-CSF timing following chemotherapy (Morstyn et al., 1989; Meisenberg et al., 1992; Butler et al., 1992; Fukuda et al., 1993; Koumakis et al., 1999), but the conclusions vary between studies. The goal of this paper is to study G-CSF treatment strategies following chemotherapy using a mathematical modeling approach and supplemented by numerical simulations.

Over the past decades, mathematical modeling has provided insight into different aspects of biological system function. Several mathematical models have been used as tools for better understanding the nature of hematopoiesis and hematopoietic diseases (see Roeder, 2006; Foley and Mackey, 2009 for reviews). Some of these models are very detailed and aimed at obtaining insight into biological mechanisms (Rubinow and Lebowitz, 1975; Shochat et al., 2002; Vainstein et al., 2005). They have several compartments and hence are often high dimensional and contain a large number of parameters. Other models focus on specific aspects of neutrophil production. These models can take various forms and present different levels of details. For instance, they could be

* Corresponding author. Tel.: +1 514 398 3047; fax: +1 514 398 7452.
E-mail addresses: foley@math.mcgill.ca (C. Foley), michael.mackey@mcgill.ca (M.C. Mackey).
[1] Tel.: 1-514-398-4336; fax. 1-514-398-7452.

0022-5193/$ - see front matter © 2008 Elsevier Ltd. All rights reserved.
doi:10.1016/j.jtbi.2008.09.043

formulated as partial differential equations (PDE) (Ostby et al., 2003), delay differential equations (DDE) (Bernard et al., 2003; Foley et al., 2006) or ordinary differential equations (ODE) (Panetta et al., 2003; Friberg et al., 2002; Scholz et al., 2005; Shochat et al., 2007).

Analysis and numerical simulations of such mathematical models can also provide a way of studying G-CSF treatment strategies in various contexts. For example, Ostby et al. (2003) proposed a reaction–diffusion PDEs model for the hematopoietic reconstitution after high-dose chemotherapy and G-CSF treatment. They investigated the physiological effects of G-CSF on proliferation rate, maturation rate, mobilization and cell death relative to engraftment. Scholz et al. (2005) used an ODE model for computing the time dependent behavior of cell numbers in each compartment under the influence of poly-chemotherapy and G-CSF administration. Their model includes self-regulating mechanisms that describe the effects of G-CSF administration and chemotherapy treatment. Shochat et al. (2007) developed a simple two-dimensional ODE system for the G-CSF-neutrophil dynamics using an axiomatic approach. They performed a detailed mathematical analysis to deduce interesting dynamical properties of the system. Finally, Foley et al. (2006) and Colijn et al. (2007) used DDE models to propose alternative G-CSF treatment schedules for cyclical neutropenia. However, in their models, G-CSF effects were implicitly included through negative feedback functions.

The model we develop in this paper is a four-dimensional DDE model coupled with a two-compartment ODE model that accounts for G-CSF subcutaneous administration. It is distinguished from previous DDE models by an explicit modeling of the effects of G-CSF administration on amplification, maturation and apoptosis rates. Moreover, the model can reproduce currently available clinical data for two forms of recombinant G-CSF used in clinical practice (filgrastim and pegfilgrastim). We use it to study alternative time schedules for G-CSF following chemotherapy as well as dynamical aspects of the system.

The paper is organized as follows. First, we review some aspects of granulopoiesis and present the standard clinical G-CSF treatment procedures following chemotherapy in Section 2. Then, in Section 3, we develop a new mathematical model for neutrophil production that accounts explicitly for G-CSF effects. This model is then used in Section 4 to numerically study alternative G-CSF schedules for two forms of G-CSF (filgrastim and pegfilgrastim). In Section 5, we study some dynamical properties of the model and conclude with a discussion in Section 6.

2. Background

In this section, we review the basic aspects of granulopoiesis and discuss how G-CSF is used for treating chemotherapy-induced neutropenia. We also briefly review previous clinical attempts in optimizing G-CSF treatment schedules following chemotherapy in Section 2.2.3.

2.1. Granulopoiesis

Granulopoiesis is the term for the production of granulocytes. Neutrophils are the most abundant type of granulocytes. Neutrophil precursors in the bone marrow can be divided into two pools: the mitotic and the post-mitotic pools. Cells in the mitotic pool are proliferative and they consist of the progenitor cells, myeloblasts, promyelocytes and myelocytes. Cells in the post-mitotic pool are non-proliferative and they act as a reserve pool (or storage compartment) before entering the blood. They consist of metamyelocytes and the banded and segmented neutrophils. Under normal physiological conditions, the transit time through the mitotic pool is approximately 6 days (Israels and Israels, 2002). Then, cells are held in the bone marrow in the post-mitotic pool for about another 6 days (Price et al., 1996) before being released into the circulation. When G-CSF levels are increased (either in response to an inflammatory process or by exogenous administration), the transit times through the mitotic and post-mitotic pools are reduced (Lord et al., 1989). G-CSF acts on both precursor and mature cells by stimulating the effective proliferation of committed granulocytes progenitors (myeloblasts, promyelocytes and myelocytes), apparently by decreasing apoptosis. Administration of exogenous G-CSF is known to increase the number of circulating neutrophils by increasing the number of mitotic cells, reducing the maturation time and releasing the bone marrow storage pool (Israels and Israels, 2002; Lord et al., 1989; Price et al., 1996).

2.2. Treating neutropenia using G-CSF treatment

G-CSF is a hematopoietic growth factor that stimulates the bone marrow to increase the production of neutrophils. Thus, this is the treatment of choice for neutropenia. It is produced naturally in the body, but recombinant forms of G-CSF (filgrastim (Neupogen), lenograstim (Granocyte) and pegfilgrastim (Neulasta)) are used as drugs to accelerate recovery from neutropenia. In this study, we will only consider filgrastim and pegfilgrastim. They are both G-CSF analogs produced by recombinant DNA technology. The gene for human G-CSF is inserted into the genetic material of *Escherichia coli*. Recombinant G-CSF produced by *E. coli* is only slightly different from G-CSF naturally made in humans. Filgrastim is a small molecule which is rapidly filtered by the kidney and cleared from the blood, necessitating daily administrations. The pegylated filgrastim (pegfilgrastim) is the same molecule as filgrastim but to which a 20 kDa polyethylene glycol moiety has been added. This addition changes its pharmacokinetic properties and virtually eliminates renal clearance. Hence, whereas filgrastim is rapidly cleared after a subcutaneous dose, pegfilgrastim, a bigger molecule, has a much longer half life. Therefore, only a single administration after each cycle of chemotherapy is necessary for pegfilgrastim instead of a number of daily injections for filgrastim, thereby reducing cost and inconvenience to the patient.

Other than a difference in their clearance rate, both molecules have the same effects: they boost the number of neutrophils by decreasing the apoptosis rates in neutrophil precursors (Hannun, 1997) and thus increasing the effective amplification factor, and accelerating the transit time through the postmitotic pool (Lord et al., 1989; Price et al., 1996).

2.2.1. Side effects

Even though G-CSF is a natural substance, a too high concentration can cause side effects such as bone pain, red and itchy skin, fever, chills and fluid retention, nausea, vomiting and diarrhea.

2.2.2. Clinical uses

G-CSF is used clinically to treat neutropenia in several situations. In particular, since a common side effect of many chemotherapeutic drugs is a reduction in the number of WBCs, G-CSF is often given after chemotherapy to elevate the WBC production. It is usually given subcutaneously (injection under the skin) because the increase in neutrophil count is higher and the stimulated duration is longer than with an intravenous administration of the same dose (Hayashi et al., 2001). In this study, we only consider the use of G-CSF following myelosuppressive chemotherapy on patients suffering from non-myeloid types of

cancer, e.g. we are assuming that a model of regulation of neutrophil production can be taken to represent a hematologically normal individual.

Filgrastim (Neupogen)'s clinical guidance (www.neupogen.com) for cancer patients receiving myelosuppressive chemotherapy recommends a starting dose of 5 μg/kg/d, subcutaneously. Doses may be increased in increments of 5 μg/kg for each chemotherapy cycle, according to the duration and severity of the ANC nadir. Typically, a rapid rise in the neutrophil count is observed after G-CSF administration, followed by a neutrophil decrease to low ANC values. After this ANC nadir, the neutrophil levels then increase. Neupogen should be administered no earlier than 24 h after the administration of cytotoxic chemotherapy and it should be administered daily for up to 2 weeks, until the ANC has reached normal levels following the expected chemotherapy-induced neutrophil nadir.

The recommended dosage of Neulasta (pegfilgrastim) is a single subcutaneous injection of 6 mg administered once per chemotherapy cycle (clinical guidances www.neulesta.com). Neulasta should not be administered in the period between 14 days before and 24 h after administration of cytotoxic chemotherapy.

2.2.3. Previous studies on G-CSF administration

In this section, we review previous clinical attempts to optimize filgrastim administration following chemotherapy.

The use of G-CSF has been proven to be of great utility in reducing chemotherapy-induced neutropenia. Nevertheless, it is not clear what would be the best schedule for giving G-CSF following chemotherapy. A few studies have considered alternative G-CSF regimens in order to find optimal G-CSF timing (Morstyn et al., 1989; Meisenberg et al., 1992; Butler et al., 1992; Fukuda et al., 1993; Koumakis et al., 1999). However, the results and conclusions vary from one study to another. There are basically two main lines of thought concerning the timing of G-CSF administration. Some authors consider that the duration of neutropenia and the neutrophil nadir are not significantly different whether G-CSF is given as early as 24 h or even as late as 8 days after chemotherapy (Meisenberg et al., 1992; Morstyn et al., 1989). However, others have concluded that it is preferable to start G-CSF administration early after chemotherapy treatment because it reduces the number of infections and hospitalization days. Next, we briefly discuss the main results of studies based on these two premises.

In their study on monkeys, Meisenberg et al. (1992) showed that beginning daily filgrastim (5 μg/kg) on either days 1, 3, 5 or 7 after chemotherapy all reduce neutropenia. They demonstrated that the duration of G-CSF treatment could be reduced considerably by delaying G-CSF initiation. They also observed that early G-CSF (1 day after chemotherapy) led to a more rapid recovery of myeloid progenitor cells and an earlier onset of neutropenia than delayed treatment.

Morstyn et al. (1989) also studied the effects of delaying filgrastim treatment following chemotherapy and of reducing its duration of administration. Data in their paper suggests that the amplitude in the ANC levels in response to G-CSF could vary depending on the starting day of G-CSF administration. In particular, maximal neutrophil levels are higher when starting filgrastim treatment on the day following chemotherapy and lower when starting 7 days after chemotherapy. Morstyn et al. (1989) demonstrated that starting G-CSF 7 days after chemotherapy still has the effect of rapidly raising the ANC levels, although the neutrophil response is typically of smaller amplitude. They also concluded that it was not necessary to continue G-CSF for more than 7 days.

In contrast to these studies, Butler et al. (1992) administered G-CSF starting on days 4 or 11 during intensive chemotherapy for breast cancer. They found that patients who were given G-CSF on day 4 had fewer days of neutropenia, hospitalization and antibiotic days while having similar duration the G-CSF treatment. These results are in agreement with another study by Fukuda et al. (1993), who also showed that early G-CSF administration following chemotherapy was more beneficial than late administration, when the number of neutropenic days and the depth of the nadir were considered.

Finally, Koumakis et al. (1999) compared various timing schedules of G-CSF treatment following chemotherapy. They were interested in investigating the dependence of the optimal time (preemptive vs. supportive) of G-CSF initiation on criteria such as incidence of febrile neutropenia, antibiotic use, duration and cost of G-CSF administration. Preemptive treatment involves starting G-CSF shortly after chemotherapy whereas in supportive therapy, G-CSF is started later and only when neutropenia occurs. The authors concluded that G-CSF administration shortens neutropenia regardless of the treatment starting day and that no significant difference was observed among early- and late- treatment groups. However, the incidence of antibiotic use and febrile episodes was less when G-CSF was started early (1 or 2 days after chemotherapy). For these reasons, they recommended preemptive rather than therapeutic administration of G-CSF for subjects receiving chemotherapy.

3. Mathematical model

In this section, we describe a mathematical model for neutrophil regulation and production. This model is divided into two parts: the main compartment, which models the WBC production system, and the G-CSF compartment, which models G-CSF subcutaneous injections. The effects of G-CSF are included in the main compartment through different functions. This model will be used in Section 4 to study the effects of different schedules of G-CSF following chemotherapy.

3.1. Description of the main part of the model

We consider a model with five compartments. Let $m(t,a)$, $s(t,a)$, $p(t,a)$, $n(t,a)$ and $w(t,a)$ be the population densities at time t and age a of proliferative stem cells, resting (G_0) stem cells, proliferative precursors cells, non-proliferative precursors and circulating WBCs, respectively (see Fig. 1). We make the following assumptions:

1. *Apoptosis*: We assume that in each of these compartments (except for the G_0 stem cell compartment), there is a random loss of cells due to apoptosis, at a rate denoted by $\gamma_s, \gamma_p, \gamma_n$ and γ_w for the proliferative stem cells, proliferative precursors, non-proliferative precursors and circulating neutrophils, respectively. We assume that all of the apoptosis rates except γ_w depend on the G-CSF concentration $G(t)$. Since G-CSF inhibits the chemotherapy-induced apoptosis (see Appendix C.1), we will mimic the action of G-CSF following chemotherapy by decreasing the apoptosis rates γ_S, γ_p and γ_N as a function of G-CSF. We use the following decreasing bounded functions:

$$\gamma_s(G) = (\gamma_s^{max} - \gamma_s^{min})\frac{b_s}{G + b_s} + \gamma_s^{min}, \tag{1}$$

$$\gamma_p(G) = (\gamma_p^{max} - \gamma_p^{min})\frac{b_p}{G + b_p} + \gamma_p^{min}, \tag{2}$$

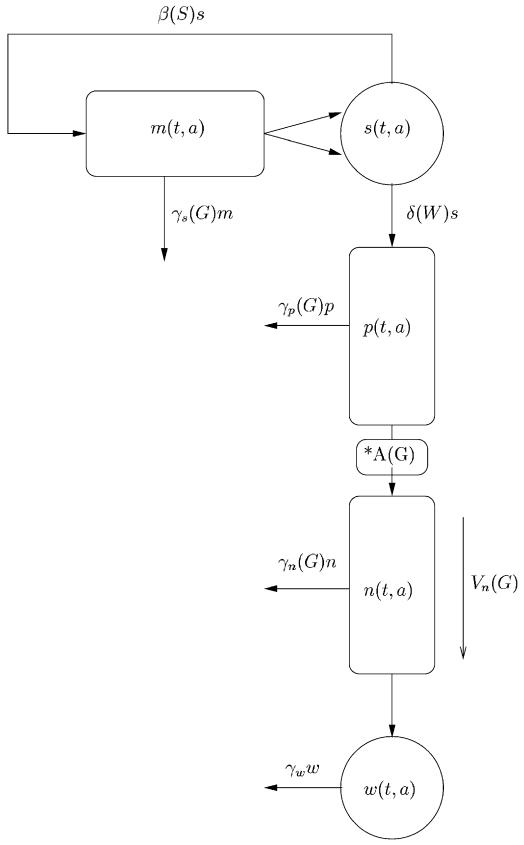

Fig. 1. Schema of the main part of the model. See the text for full details as well as the notation.

$$\gamma_n(G) = (\gamma_n^{max} - \gamma_n^{min})\frac{b_n}{G + b_n} + \gamma_n^{min}, \tag{3}$$

where γ_i^{min} and γ_i^{max} are, respectively, the minimum and maximum values for the apoptosis rates ($i = s, p, n$) and the b_i are parameters that control the steepness of the function.

2. *Aging velocity*: We assume that the cells in each compartment age with a certain velocity $V_i(G), i = m, s, p, n, w$. In particular, we take V_m (proliferative stem cells), V_s (stem cells in G_0 phase), V_p (proliferative precursors) and V_w (WBCs) to be equal to 1. On the other hand, we consider that the velocity for the non-proliferative precursors compartment ($V_n(G)$) depends explicitly on G-CSF because G-CSF is known to modify the maturation time of this population (Lord et al., 1989). We assume that a cell enters the non-proliferative compartment at age $a = 0$ and exits this compartment at age $a = \tau_n$. Hence, if we increase $V_n(G)$, the transit time through that phase will decrease since it will take less time to go through the compartment. The aging velocity is related to the transit time through a given stage. Since we do not have any a priori information on how G-CSF decreases the time spent in the non-proliferative precursor phase, we use a simple bounded relationship:

$$V_n(G) = (V_{max} - 1)\frac{G}{G + b_v} + 1. \tag{4}$$

Note that this function is increasing so that the time spent in the phase is decreased as G increases.

3. *Differentiation rate*: We assume that the differentiation rate $\delta(W)$ from the resting G_0 stem cell compartment to the proliferative phase depends on the number of circulating neutrophils $W(t)$. We use the same decreasing function as in Colijn and Mackey (2005) ($\delta(W) = f_0(\theta_1/\theta_1 + W)$). Hence, when the neutrophil count is low, it increases the differentiation rate $\delta(W)$.
4. *Re-entry of G_0 phase stem cells into proliferation*: Cells in the resting G_0 phase (represented by $s(t, a)$) can either differentiate at a rate $\delta(W)$ or reenter proliferation at a rate $\beta(S)$ (we will assume β does not depend on $G(t)$). The function $\beta(S)$ is a decreasing Hill function ($\beta(S) = k_0(\theta_2^2/\theta_2^2 + S^2)$). Hence, as the number of cells in the G_0 phase decreases, the proliferation rate is increased. Cells enter the proliferative phase of the stem cells at age $a = 0$ and leave at age $a = \tau_s$. We assume that before entering the G_0 compartment, the cells divide into two daughter cells and hence we consider an amplification factor of 2.
5. *Amplification factor $A(G)$*: Cells exiting the proliferative phase are amplified by a factor $A(G)$. This accounts for the number of divisions occurring in the proliferative phase and it depends on the G-CSF concentration explicitly. Again, as we have no a priori information on its shape, we assume a bounded relationship:

$$A(G) = (A_{max} - A_{min})\frac{G}{G + b_A} + A_{min}. \tag{5}$$

From Fig. 1, one can derive a set of PDEs. Using the method presented in Foley and Mackey (2009), we can integrate each equation and express the model as DDEs for the total cell population numbers $S(t)$, $P(t)$, $N(t)$ and $W(t)$. The complete derivation of the PDE and DDE models are presented in Appendix A and yields the following DDEs system:

$$\frac{dS}{dt} = 2\beta(S_{\tau_s})S_{\tau_s}\exp\left(\int_0^{\tau_s} -\gamma_s(G(t))\,dt\right) - [\beta(S) + \delta(W)]S, \tag{6}$$

$$\frac{dP}{dt} = -\gamma_p(G)P + \delta(W)S - \delta(W_{\tau_p})S_{\tau_p}\exp\left(-\int_0^{\tau_p}\gamma_p(G(t))\,dt\right), \tag{7}$$

$$\begin{aligned}\frac{dN}{dt} = &-\gamma_n(G)N + V_n(G)\delta(W_{\tau_p})S_{\tau_p}\exp\left(-\int_0^{\tau_p}\gamma_p(G(t))\,dt\right)\\ &\times\left[A(G) - A(G_{\tau_n^-}) * \exp\left(-\int_0^{\tau_n^-}\gamma_n(G(t))\,dt\right)\right],\end{aligned} \tag{8}$$

$$\begin{aligned}\frac{dW}{dt} = &-\gamma_w W + A(G_{\tau_n^-})\delta(W_{\tau_p})S_{\tau_p^-}\\ &\times\exp\left(-\int_0^{\tau_p}\gamma_p(G(t))\,dt - \int_0^{\tau_n^-}\gamma_n(G(t))\,dt\right).\end{aligned} \tag{9}$$

A subscript on a variable denotes a temporal delay in that variable ($x_\tau := x(t - \tau)$).

3.2. Description of the G-CSF model

As it can be seen from the previous equations, many of the parameters in the system depend on the G-CSF concentration $G(t)$. Indeed, G-CSF regulates the system in several different ways and, in particular, it is known to regulate the neutrophil production through a negative feedback mechanism.

The model for G-CSF is similar to the one used in Colijn et al. (2007). It is a two-compartment model that accounts for subcutaneous G-CSF injections. The model is illustrated in Fig. 2. The notation is as follows: X denotes the tissue levels of G-CSF (units μg/kg(body weight)) and G denotes the circulating G-CSF concentration (units μg/mL). Note that instead of using concentrations for both tissue and blood compartment, we used per body weight levels for the tissue compartment. Since it is easier to express the input $I(t)$ in terms of quantity, this allows us to get rid of the parameter representing the volume of tissue compartment.

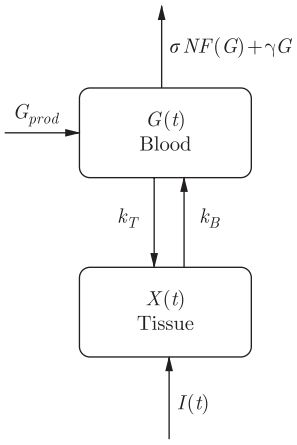

Fig. 2. A two-compartment model for subcutaneous administration of G-CSF. $I(t)$ is a step function representing injection of exogenous G-CSF into the tissues. $X(t)$ and $G(t)$ are, respectively, the amount of G-CSF in tissues (μg/kg) and the blood G-CSF concentration (μg/mL). k_T and k_B are rate constants for exchange between the blood and tissue compartments. G-CSF clearance rate is given by $\sigma NF(G)+\gamma_G$. See the text for further details.

Of course, the corresponding terms need to be scaled accordingly by the volume of the blood compartment V_B in order to make units of G and X agree in both equations. G-CSF is injected into the tissue compartment and enters the circulation from there. It is eliminated through saturable and unsaturable mechanisms. The saturable mechanism involves the G-CSF receptors on neutrophils whereas the unsaturable process mainly involves kidneys.

From Fig. 2, one can write down the dynamic equation for the G-CSF compartment:

$$\frac{dX}{dt} = I(t) + k_t V_B G - k_B X, \tag{10}$$

$$\frac{dG}{dt} = G_{prod} + \frac{k_B X}{V_B} - k_T G - (\gamma_G + \sigma WF(G))G. \tag{11}$$

The first equation represents the rate of change of G-CSF in tissues. $I(t)$ is the input from exogenous G-CSF given subcutaneously, V_B is the volume of the blood compartment and k_T and k_B are rate constants for exchange between the blood and tissue compartments. The rate of change of G-CSF concentration in blood is expressed in the second equation, where G_{prod} is the fixed G-CSF production and the clearance is given by $\gamma_G G + \sigma WF(G)G$.

Next, we derive expressions for G-CSF clearance and the input function $I(t)$ that models subcutaneous injections.

3.2.1. G-CSF clearance

A number of mathematical models of G-CSF clearance have been used in the literature. Some authors used Michaelis–Menten kinetics to model the combination of saturable and non-saturable clearance (Kuwabara et al., 1994; Hayashi et al., 2001; Ostby et al., 2003). Alternatively, one could model the unsaturable clearance by a first-order process and the saturable G-CSF clearance by directly treating the binding of G-CSF receptors (Vainstein et al., 2005). The model we propose here is of the second type.

First, the unsaturable clearance process could be modeled by a first-order process $\gamma_G G$, where γ_G is the rate of degradation of G-CSF by the kidneys. To this, we add an expression for the saturable G-CSF clearance. Indeed, G-CSF is also removed from the circulation by binding to free receptors on neutrophils. Let $F(G)$ be the fraction of bound G-CSF receptors, W be the neutrophil number and σ be a binding coefficient of G-CSF to its receptors. Thus, the number of G-CSF molecules removed from the circulation through the saturable clearance is given by $\sigma WF(G)$, where

$$F(G) = \frac{G^2}{G^2 + k}. \tag{12}$$

The reader is referred to the appendix for further details on the derivation of the function $F(G)$.

3.2.2. Input function $I(t)$

In this study, we consider subcutaneous administration of rhG-CSF, which has been shown to lead to a higher increase in neutrophil count and a longer duration than for intravenous administration (Hayashi et al., 1999). To model a bolus subcutaneous injection (a high quantity of drug injected rapidly in the tissue), we used a step function of amplitude a and duration s that is turned on at $t = t_{on}$. More precisely,

$$I(t) = a * [H(t - t_{on}) * (1 - H(t - (t_{on} + s)))], \tag{13}$$

where $H(t)$ is the heaviside function defined as

$$H(t) = \begin{cases} 0, & t \leqslant 0, \\ 1, & t > 0. \end{cases}$$

The total quantity given in the bolus injection is easily computed as $a * s$.

4. Numerical simulations

In this section, we numerically integrate the mathematical model and study the effects of two forms of G-CSF (filgrastim and pegfilgrastim) following chemotherapy. For more details about the numerical methods, the reader is referred to Appendix D.

4.1. Simulating filgrastim effects following chemotherapy

The use of cytotoxic drugs is considered as a standard treatment for cancer. There are many chemotherapeutic agents and several of them have been shown to induce apoptosis in cancer cells as well as in healthy cells (see Hannun, 1997 for a review). Moreover, the apoptosis induced by cytotoxic agents can be inhibited by hematopoietic growth factors, such as G-CSF (Lotem and Sachs, 1992). In this section, we use the model to study the effects of daily G-CSF (filgrastim) on subjects suffering from non-myeloid malignancies who have undergone chemotherapy. First, we present the numerical method used for simulation in Section 4.1.1. Then, we use our model to study the effects of the starting day of G-CSF treatment following chemotherapy (Section 4.1.2) and of the duration of G-CSF treatment (Section 4.1.3).

4.1.1. Numerical method

From a modeling point of view, the effects of chemotherapy and G-CSF treatment are mimicked through the functions $A(G), V_n(G), \gamma_s(G), \gamma_p(G)$ and $\gamma_n(G)$. As explained in Section 3, G-CSF increases the amplification factor, decreases the transit time in the postmitotic pool (increases aging velocity V_n) and decreases the apoptosis rates in the stem cells (γ_S) and in the neutrophil precursor cells (γ_N and γ_P).

To numerically simulate the effects of G-CSF following chemotherapy, we start from the stable steady state found that represents cancer (Appendix D.1). Then, we increase the values of γ_s, γ_p and γ_n to their maximum values γ_i^{max} $(i = s, p, n)$ to mimic the effects of chemotherapy. The administration of exogenous G-CSF is explicitly expressed by changing the input function $I(t)$, which then affects the amplification $A(G)$, the aging velocity $V_n(G)$ and the apoptosis rates $\gamma_s(G), \gamma_p(G)$ and $\gamma_n(G)$. The parameters used

after chemotherapy are the same as in healthy/cancer subjects (Appendix D.2). Finally, note that since it is recommended that G-CSF be started at least 24 h after chemotherapy, we gradually decrease the apoptosis rates between the end of chemotherapy and the beginning of G-CSF treatment. We use decreasing linear functions of the type $\gamma_i(t) = (\gamma_i^{min} - \gamma_i^{max})t/8 + \gamma_i^{max}$ for $i = s, p, n$. The factor 8 in the slope of the linear functions was chosen because a study in monkeys (Meisenberg et al., 1992) reported an average period of 8 days for recovery of the ANC following chemotherapy.

In the next sections we use our model to study the timing of filgrastim administration with respect to the starting day of administration and the duration of treatment.

4.1.2. Effects of varying the starting day of filgrastim treatment

As discussed above, it has been suggested that delayed initiation of filgrastim could successfully reduce neutropenia while being cost-effective. Using our mathematical model, we found that changing the starting day of filgrastim administration could result in important qualitative changes in the ANC levels. Fig. 3 shows the effects of starting filgrastim 1 day and 8 days after chemotherapy. Note that, as in Morstyn et al. (1989), our model leads to very different responses in the ANC levels. Early administration of filgrastim results in a large response in the neutrophil levels, followed by a decrease to low ANC. Filgrastim was simulated to stop when the neutrophil levels were back to normal following this nadir. Conversely, initiation of filgrastim 8 days after chemotherapy lead to a very different qualitative response. Neutrophil levels increased but remained relatively stable around normal levels during G-CSF treatment without falling to very low values (see Fig. 3). Starting G-CSF one week after chemotherapy leads to a reduced maximum ANC during G-CSF treatment (about half of the maximum ANC value when starting G-CSF the day following chemotherapy) (see Fig. 4). Interestingly, delaying filgrastim of one week also coincides with higher neutrophil nadir during filgrastim treatment (approximately twice the nadir value compared to starting treatment on day one). These results are in agreement with those reported in Morstyn et al. (1989). They suggest that late G-CSF administration following chemotherapy should be efficient in reducing the neutropenic period, *provided* that neutropenia does not occur prior to the start of treatment. However, this solution is not suitable if the neutrophil levels are very low between the end of chemotherapy and the starting day of G-CSF treatment. Since the ANC increases rapidly after filgrastim administration, these results also suggest that filgrastim could be efficiently used as supportive treatment, i.e. starting G-CSF only at the onset of neutropenia. Moreover, this could result in a more stable ANC response and avoid the typical decrease in neutrophil count.

However, we do not take into account the use of antibiotics in this model, which is a criterion that was in favor of a preemptive treatment in the study by Koumakis et al. (1999). Also, in a clinical setting, there are several factors to consider when administering G-CSF to patients, such as the type of cancer, the intensity of the chemotherapy, the age and general health of the subject, the history of febrile neutropenic episodes, etc. All these factors can influence the response to filgrastim treatment. Therefore, our results should be looked at from a qualitative point of view. Our model suggests that two different types of response (large amplitude followed by low nadir and a relatively stable ANC) can be obtained by filgrastim administration. We believe that this may be due to the existence of multiple stable solutions in the system (see Section 5). In conclusion, modifying the initiation of treatment after chemotherapy could be beneficial. Indeed, since the primary goal of G-CSF administration is to reduce the number of days where severe neutropenia occurs, the fact that changing the starting day of filgrastim can lead to higher ANC nadir and avoid the typical decrease in neutrophil count is certainly a great improvement.

4.1.3. Effects of varying the duration of filgrastim treatment

In this section, we study the effects of varying the duration of filgrastim treatment. Since clinical guidelines suggest starting filgrastim on day 1 and stopping its administration when the neutrophil levels are back to normal values following the expected nadir, we chose to always simulate the start of filgrastim on the day following chemotherapy and only vary the end of G-CSF treatment.

Fig. 5 shows the simulation when filgrastim is given for 4, 8 and 12 days. When starting treatment on day 1, one can see that a

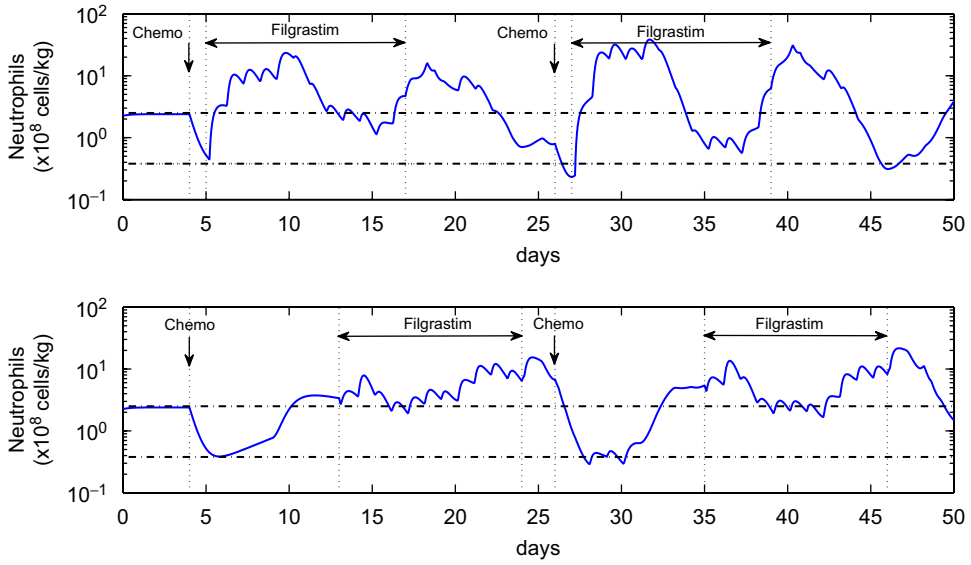

Fig. 3. Simulation of two cycles of chemotherapy and daily filgrastim (5 μg/kg). Top panel: filgrastim is administered daily, starting the day following chemotherapy treatment until the neutrophil levels reach normal values following the expected nadir. Bottom panel: filgrastim is started 8 days after chemotherapy treatment for a period of 11 days. Changing the starting day of treatment can lead to different responses in the neutrophil count. The two black dotted lines indicate the level for severe neutropenia (0.38×10^8 cells/kg) and a normal neutrophils level (2.5×10^8 cells/kg).

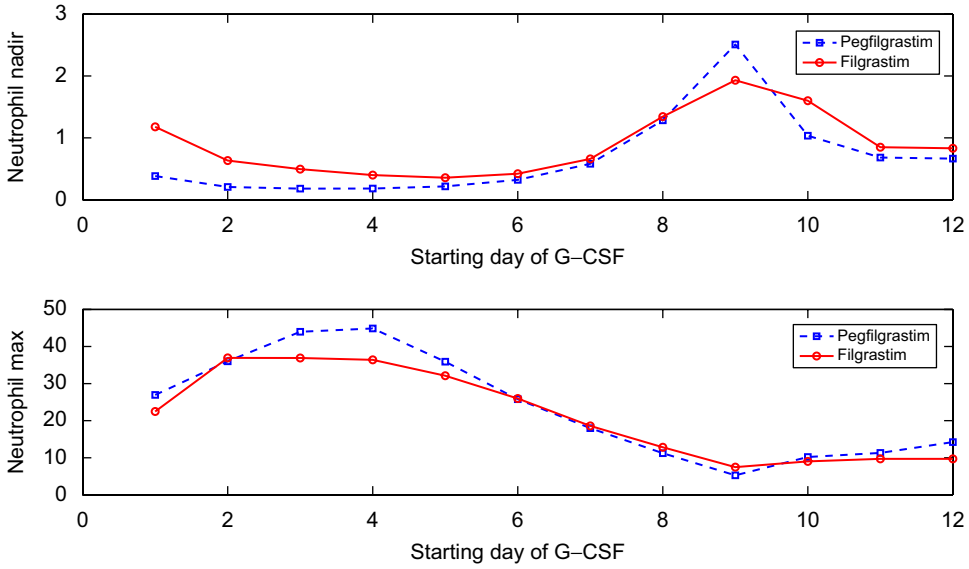

Fig. 4. Minimum and maximum neutrophil values during G-CSF treatment for both filgrastim (5 μg/kg/day) and pegfilgrastim (100 μg/kg) with respect to the starting day of G-CSF treatment following chemotherapy. Neutrophil levels are in $\times 10^8$ cells/kg.

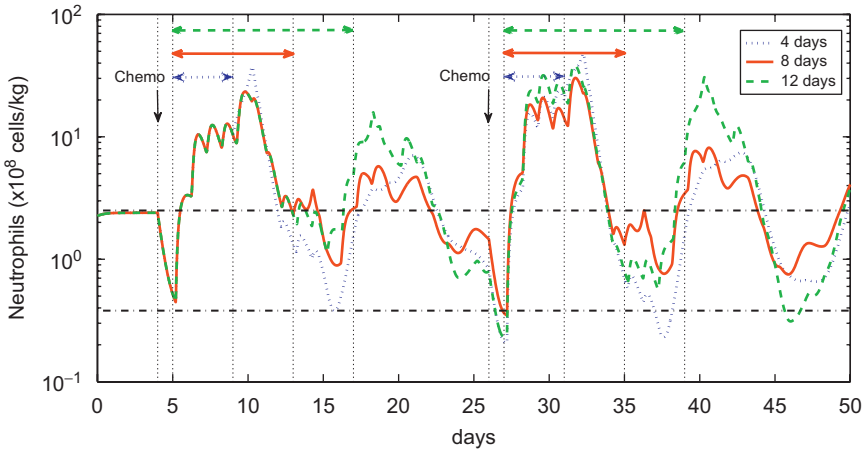

Fig. 5. Effects of varying the duration of filgrastim treatment. Simulation of daily filgrastim (5 μg/kg) started on day 1 after chemotherapy. Top panel: filgrastim is given for 4 days and stopped when the ANC is still increasing. Middle panel: filgrastim is given for 8 days and stopped just before the nadir. Bottom panel: the duration of filgrastim is 12 days and filgrastim is stopped when neutrophil levels have reached normal ANC after the expected nadir. The two black dotted lines indicate the level for severe neutropenia (0.38×10^8 cells/kg) and a normal neutrophils level (2.5×10^8 cells/kg).

rapid rise in neutrophil occurs, followed by the decrease and a second increase in ANC. The amplitude of this second increase as well as the depth of the expected nadir vary with the length of treatment. For each duration of filgrastim from 1 to 14 days, we computed the nadir and maximum neutrophil counts of the second ANC increase over two cycles of chemotherapy (see Fig. 6). We found that the longer the treatment, the higher are the maximum neutrophil levels. More interestingly, depths of the nadir are similar for treatment duration of more than 8 days. With this model, administering filgrastim for 8 days correspond to stopping it just before the expected neutrophil nadir whereas ending G-CSF when ANC are back to a normal after the nadir corresponds to a duration of 12 days of treatment. Therefore, our simulations suggest that the duration of filgrastim therapy could be reduced by stopping treatment when the nadir is reached, instead of waiting for the ANC to get back to normal levels. This reduction in the amount of filgrastim would not only reduce the cost of treatment and the side-effects due to filgrastim, but also be as effective as the current treatment scheme.

It is worth noting that only one day of filgrastim given the day following chemotherapy leads to a reduced increase of the ANC and a higher neutrophil nadir, as shown in Fig. 7. As in the case of delayed treatment discussed above, the ANC response remains relatively stable around normal values, without falling down to very low neutrophil levels. We make the hypothesis that this reflects the existence of another stable solution in the system. From a mathematical point of view, many factors influence the response of the model, among which the historical values of all variables (stem cells, precursors, neutrophils) as well as the choice of parameters. Therefore, even though our model predicts the existence of such solution and suggests that only one day of filgrastim could be successful in managing chemotherapy-induced neutropenia, further investigation would be needed since, to our knowledge, no data on this are available in the literature.

As one can see in Fig. 6, the nadirs and maximum values with respect to the duration of treatment have similar behavior for both cycles, except that the nadirs are lower and maximums are higher for the second cycle. We do not have a clear explanation for

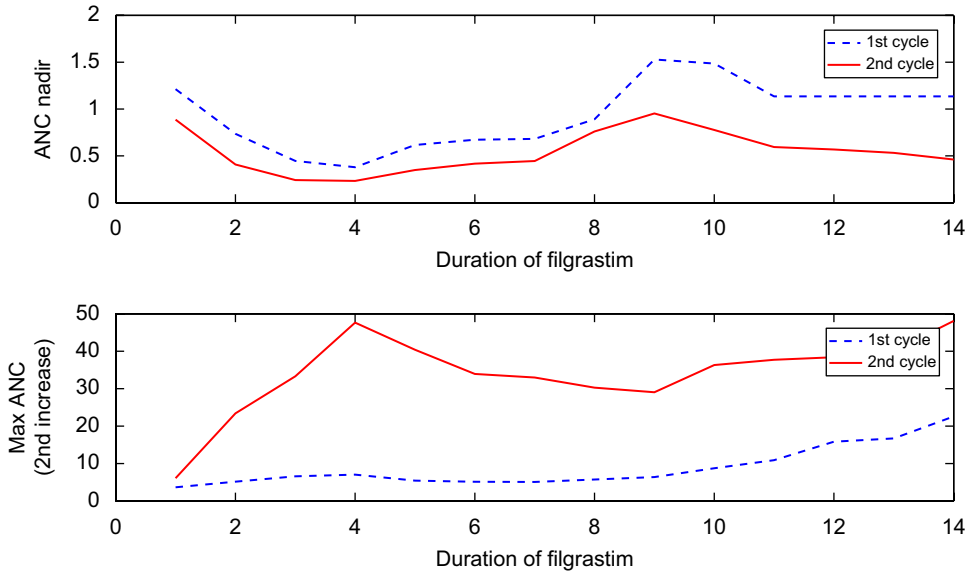

Fig. 6. Effects of the duration of daily filgrastim (5 μg/kg) over two cycles of chemotherapy (3 weeks between chemotherapy treatment). Filgrastim is started on day 1. Top panel: values of the chemotherapy-induced nadir with respect to the duration of treatment. Bottom panel: Maximum neutrophil levels reached following the expected nadir. Neutrophil levels are in $\times 10^8$ cells/kg.

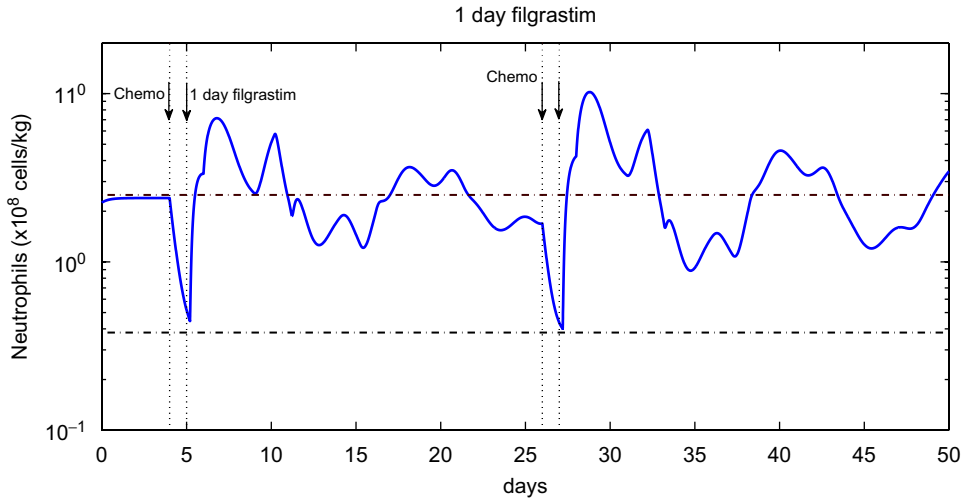

Fig. 7. Simulation of filgrastim (5 μg/kg) given only for one day the next day after chemotherapy. Two cycles of chemotherapy (3 weeks between chemotherapy treatment) are shown. ANC levels remain close to normal values and no deep nadir occurs. Neutrophil levels are in $\times 10^8$ cells/kg. The two black dotted lines indicate the level for severe neutropenia (0.38×10^8 cells/kg) and a normal neutrophils level (2.5×10^8 cells/kg).

that difference. However, since we are mainly interested in the dynamical properties of the model, we believe that this quantitative aspect is of less importance and focus on the fact that the same types of variations in nadirs and maximum values hold for both cycles.

4.2. Simulating pegfilgrastim responses following chemotherapy

In this section, we study the effects of pegfilgratim administration following chemotherapy. Recall that clinical guidance for pegfilgrastim calls for a 6 mg dose no earlier than 24 h following the chemotherapy treatment. Using the parameters listed in Table 1, we integrated the model and looked at the effects of a bolus subcutaneous administration of 100 μg/kg (corresponding to the standard 6 mg dose for a 60 kg subject). As with filgrastim, we found that modifying the starting day of the treatment can change the qualitative response of the ANC levels. This was expected since a number of studies have shown that pegfilgrastim has the same effects as filgrastim for treating neutropenia (Holmes et al., 2002; Green et al., 2003; Molineux et al., 1999). Our model agrees with that. In the first panel of Fig. 8, pegfilgrastim is given 1 day after the chemotherapy treatment, resulting in a large ANC response. In the second panel, pegfilgrastim is administered 8 days (first cycle) and 5 days (second cycle) after the chemotherapy treatment. The ANC increase is of less amplitude in the first cycle. Thus, as for filgrastim, the model predicts that delaying G-CSF administration can result in different qualitative behaviors (see Fig. 4 for the minimum and maximum values with respect to the starting day of G-CSF) and potentially abolish the nadir typically observed after the large ANC rise. This also suggests that if neutropenia does not occur right after chemotherapy, delaying G-CSF treatment would be efficient while being cost-effective (Morstyn et al., 1989 reported data of such situation).

Table 1
Parameters of the model (steady state values).

Parameter name	Value used	Unit	Sources
Stem cell compartment			
S_*	1.1 (0.0001–1.1)	$\times 10^6$ cells/kg	Mackey (2001)
γ_s	0.05 (0.01–0.20)	days^{-1}	Bernard et al. (2003)
γ_s^{min}	0.05	days^{-1}	Calculated
γ_s^{max}	0.20	days^{-1}	Calculated
b_s	0.01	–	Calculated
τ_s	2.8 (1.4–4.2)	days	Bernard et al. (2003)
k_0	8.0 (2.0–10.0)	days^{-1}	Colijn and Mackey (2005)
θ_2	0.3	$\times 10^6$ cells/kg	Colijn and Mackey (2005)
f_0	0.40	days^{-1}	Colijn and Mackey (2005)
θ_1	0.36 (0.1–2.0)	$\times 10^8$ cells/kg	Colijn and Mackey (2005)
Prolif. precursors compartment			
P_*	2.11	$\times 10^9$ cells/kg	Dancey et al. (1976)
γ_p	0.27	days^{-1}	Mackey et al. (2003)
γ_p^{min}	0.27	days^{-1}	Mackey et al. (2003)
γ_p^{max}	0.45	days^{-1}	Calculated
b_p *(filgrastim)*	0.05	–	Fit
b_p *(pegfilgrastim)*	1	–	Fit
τ_p	5	days	Israels and Israels (2002)
A_{max}	20 972	100	Bernard et al. (2003)
A_{min}	655	100	Bernard et al. (2003)
b_A *(filgrastim)*	0.35	–	Fit
b_A *(pegfilgrastim)*	1.05	–	Fit
Non-prolif. precursors compartment			
N_*	5.59	$\times 10^9$ cells/kg	Dancey et al. (1976)
γ_n	0.27	days^{-1}	Mackey et al. (2003)
γ_n^{min}	0.27	days^{-1}	Mackey et al. (2003)
γ_n^{max}	0.45	days^{-1}	Calculated
b_n *(filgrastim)*	0.05	–	Fit
b_n *(pegfilgrastim)*	1	–	Fit
τ_N	6 (3.27–8.4)	days	Price et al. (1996)
V_{max}	6	–	Calculated
b_v*(filgrastim)*	0.001	–	Fit
b_v *(pegfilgrastim)*	0.08	–	Fit
Neutrophils compartment			
W_*	6.9 (4.0–10.0)	$\times 10^8$ cells/kg	Abkowitz et al. (1988) and Beutler et al. (1995)
γ_w	2.4 (2.2–2.5)	days^{-1}	Bernard et al. (2003)
G-CSF compartment			
X_*	0.1	μg/kg	Colijn et al. (2007)
G_*	0	μg/ml	Colijn et al. (2007)
V_B	76	mL/kg	Hayashi et al. (2001) and Colijn et al. (2007)
G_{prod}	7.2 $\times 10^{-29}$	μg/(ml $*$ day)	Vainstein et al. (2005)
Filgrastim			
k_T	1.68	days^{-1}	Hayashi et al. (2001) and Colijn et al. (2007)
k_B	9.84	days^{-1}	Colijn et al. (2007)
σ	0.72	kg/day	Stute et al. (1992), Kearns et al. (1993) and Colijn et al. (2007)
γ_G	3.36	days^{-1}	Fit
a	1200	μg/(kg $*$ day)	(Calculated)
s	0.0083	day	(Calculated)
t_{on}	0.0083	day	(Calculated)
k	10	–	Fit
Pegfilgrastim			
k_T	0	days^{-1}	Roskos et al. (2006)
k_B	0.32	days^{-1}	Fit
σ	0.01	kg/day	Fit
γ_G	1.4	days^{-1}	Fit
a	12 048	μg/(kg $*$ day)	(Calculated)
s	0.0083	day	(Calculated)
t_{on}	0.0083	day	(Calculated)
k	0.01	–	Fit

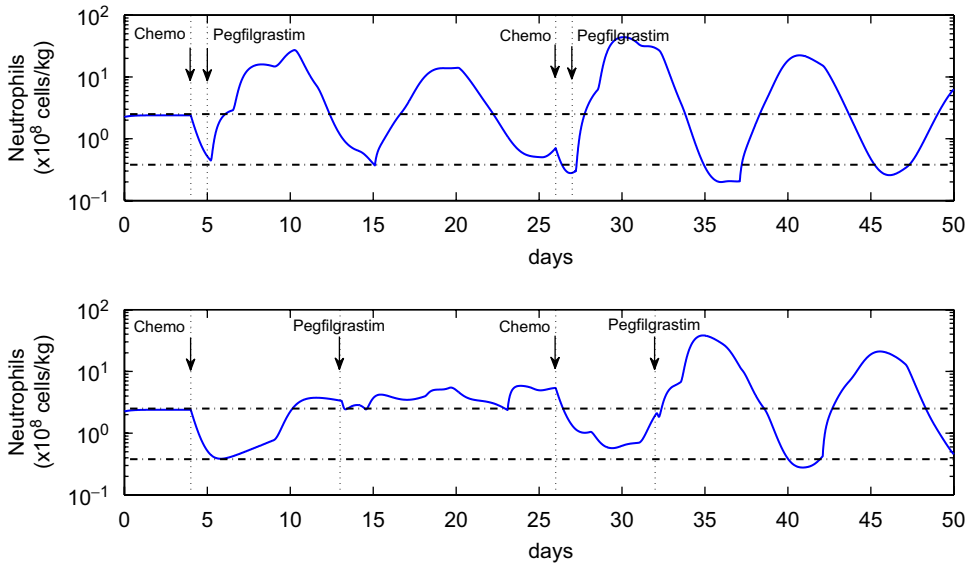

Fig. 8. Effects of changing the starting day of pegfilgrastim treatment on the neutrophil count. Top panel: pegfilgrastim (100 μg/kg) is given 1 day after chemotherapy. Bottom panel: pegfilgrastim (100 μg/kg) is given 8 days (first cycle) and 5 days (2nd cycle) after chemotherapy. The two black dotted lines indicate the level for severe neutropenia (0.38×10^8 cells/kg) and a normal neutrophils level (2.5×10^8 cells/kg).

5. Bifurcation and multistability

Numerical results from Section 4 suggest that different types of qualitative behaviors can be observed when performing simulations of the mathematical model. By varying the starting day or duration of G-CSF treatment following chemotherapy, the model displayed either a large ANC response followed by low nadir or a smaller ANC increase that remains relatively stable. We hypothesize that this is due to coexistence of multiple stable solutions (multistability) in the system. Multistability (or bistability in the case of two coexisting stable solutions) has been shown to explain different types of biological responses (Angeli et al., 2004; Ferrell, 2002; Novak and Tyson, 1993; Ozbudak et al., 2004). In particular, it has been invoked to explain the establishment of mutually exclusive phases and oscillatory behavior in cell cycle (Pomerening et al., 2003; Sha et al., 2003), properties of mitogen-activated protein kinase cascades in animal cells (Ferrell and Machleder, 1998; Bagowski and Ferrell, 2001; Bhalla et al., 2002), cell cycle regulatory circuits in *Xenopus* and *Saccharomyces cerevisiae* (Cross et al., 2002; Pomerening et al., 2003) as well as switch-like biochemical responses in the *lac* operonand *trp* operon (Yildirim and Mackey, 2003; Yildirim et al., 2004; Santillan and Mackey, 2004; Santillan et al., 2007). It has also been suggested that bistability could account for oscillations triggered by G-CSF in non-cycling forms of neutropenia (Foley et al., 2006). In this section, we study some dynamical aspects of the mathematical model in order to validate the existence of multistability.

The fact that we obtained different qualitative responses in our simulations is an indication that the system may undergo a bifurcation. A bifurcation occurs when a small change in parameter values (bifurcations parameters) causes a sudden qualitative change in the long-term dynamical behavior of the system (the reader is referred to Drazin, 1992; Perko, 2008; Beuter et al., 2003; Strogatz, 2001 for more details on bifurcation theory in dynamical systems). To better analyze the dynamical properties of the model, we first choose a relevant bifurcation parameter among all the parameters of the model. Since we are interested in the effects of G-CSF, we consider only the main part of the model (variables S, P, N, and W, see Fig. 1) and take G-CSF concentration G as the bifurcation parameter. Recall that the effects of G-CSF are modeled through the functions $A(G)$, $V_n(G)$, $\gamma_S(G)$, $\gamma_p(G)$ and $\gamma_N(G)$.

We attempted to compute a bifurcation diagram for the neutrophil level solutions with respect to G-CSF concentration G. We used `DDEBiftool`, a `matlab` package for bifurcation analysis of DDE with constant or state-dependent delays. Although the computation of steady state solutions was successful, numerical problems occurred when computing branches of periodic solutions. In fact, the system is very complex and it appears that several branches of periodic solutions (many of which are unstable) coexist. Moreover, numerical instabilities made the computation difficult.

Nevertheless, we were able to explore some dynamical aspects of the DDE model by numerically integrating the main part of the model and varying G (again considered as a parameter as explained above). We found that for low concentration of G-CSF after chemotherapy, oscillatory behavior is observed, indicating the existence of a locally stable periodic solution. Also, for large values of G-CSF concentration, solutions settled down a locally stable steady state. More interestingly, we were able to illustrate the bistable nature of the system by keeping a fixed value of G and varying only the initial function (history). We obtained two qualitatively different responses as shown in Fig. 9: a stabilization toward a locally stable steady state (top panel) and sustained oscillations (bottom panel). This shows that two coexisting stable solutions exist and may provide an explanation for the different qualitative behaviors observed in Section 4. In fact, changing the starting day of G-CSF after chemotherapy is equivalent to changing the past values of the state variables (initial functions).

6. Discussion

We have developed a mathematical model of WBC production to study schedules of G-CSF treatment following chemotherapy. The model incorporates explicitly the effects of G-CSF, namely a decrease in postmitotic transit time, an enhanced amplification, and effects on apoptosis rates. Experimental data for two recombinant forms of G-CSF, filgrastim and pegfilgrastim, were successfully reproduced with the mathematical model.

Through numerical simulations, we studied the effects of varying the starting day of G-CSF administration following chemotherapy for both filgrastim and pegfilgrastim. We found

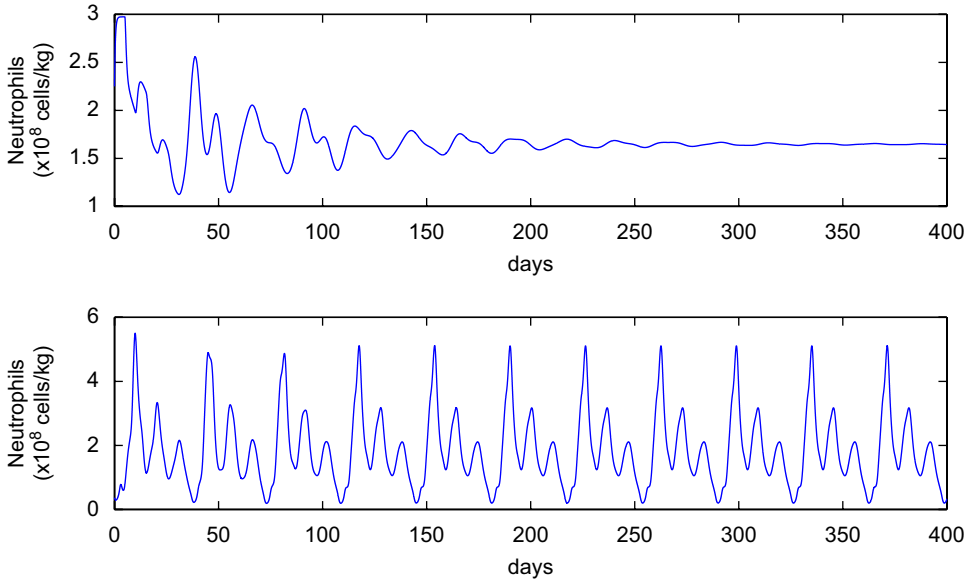

Fig. 9. Bistable behavior in the model. Simulation of the DDE model for a fixed value of $G = 0.9$. The initial functions (history) of the variables S, P, N, and W are different for each panel. Top panel: the solution settles down to a steady state. The constant initial function corresponding to steady state solutions of Section D.1 was used. Bottom panel: sustained oscillations are present, indicating the existence of a stable periodic orbit. The initial function was the oscillatory solution obtained when using $G = 0.8$ and starting with constant steady state values. Parameters used are the same as in Table 1 except that $b_i = 10$ $(i = A, v, s, p, n)$ to avoid numerical instabilities.

that this could result in two qualitatively different responses: a large neutrophil increase followed by a deep nadir (early treatment) or a smaller ANC increase that remains relatively stable and does not go to very low levels (delayed treatment). We showed that this can apparently be explained by the coexistence of two stable solutions in the system (oscillations and steady state). In fact, the model dynamics are very rich and the outcome of numerical simulations depend on several factors (parameter values, initial function, etc.). Similarly, several aspects also influence responses to G-CSF therapy in clinical practice (age, chemotherapy regimen and intensity, type of cancer, etc.). As a result, there are great variations in the ANC among individuals and also from one cycle to another for the same patient. Therefore, the reader should consider our results from a qualitative point of view and focus on the fact that changing the starting day of G-CSF could lead to different behaviors and potentially abolish the neutrophil nadir. Viewed in this light our results suggest that modifying the initiation of treatment after chemotherapy could be beneficial. Indeed, since the primary goal of G-CSF administration is to reduce the number of days where severe neutropenia occurs, the fact that changing the starting day of filgrastim can lead to higher ANC nadir and avoid the typical decrease in neutrophil count is certainly an improvement.

We also studied the effects of the duration of filgrastim treatment. Contrary to clinical guidance, which suggests administering filgrastim until ANC levels are back to normal following the expected nadir, our simulations predict that stopping it just before the nadir would have similar effects while reducing the amount of drug. This reduction in the amount of filgrastim would not only reduce the cost of treatment and the side-effects due to filgrastim, but also be as efficient as the current treatment scheme.

Earlier modeling work on alternative G-CSF schedules for cyclical neutropenia (Foley et al., 2006; Colijn et al., 2007) also suggested that different treatment regimens can lead to significantly different responses. Our results substantiate this and propose practical strategies for reducing the cost of G-CSF treatment following chemotherapy. Moreover, our model could easily be used for exploring other issues concerning G-CSF treatment. Indeed, it is easy to change the dose and the frequency of treatment in the model. One could think of other interesting treatment regimens that could be studied, such as the effects of administering G-CSF every other day, instead of everyday for example.

If enough data were available before and after chemotherapy and G-CSF treatment for a patient, a particulary interesting approach would consist of personalizing the parameters of the model. Colijn et al. (2007) proposed such an individualized modeling approach, based on data before and after G-CSF treatment from seven neutropenic dogs. The authors were able to estimate the parameters corresponding to each dog using a simulated-annealing method. Then, for each dog, they studied alternative G-CSF treatment schemes. Thus, one could think of using a similar approach with this model to estimate parameters corresponding to one patient. Optimization tools could then be used to find a suitable treatment for that patient.

The model could also be used for assessing different mechanisms of action of G-CSF. For instance, it has been shown that G-CSF increases the amplification factor for the neutrophils precursors (Lord et al., 1989). However, it is not clear whether this is due to a real increase in the number of cell divisions, a decrease in the apoptosis rate in the precursors or a combination of both. In this study, we assume both mechanisms were affected by G-CSF. Since our model accounts for these two effects separately, one could study in more detail the impact of each mechanism. In conclusion, despite the great variability among individuals, we believe that the model provides interesting insights into the effects of G-CSF treatment following chemotherapy and helps to better understand the dynamical nature of the underlying system.

Acknowledgements

This work was supported by the Natural Sciences and Engineering Research Council (NSERC, Canada), the Mathematics or Information Technology and Complex Systems (MITACS,

Canada), Fonds de Recherche sur la Nature et les Technologies (FQRNT, Canada) and Institut des Sciences Mathématiques (ISM, Canada).

Appendix A. Derivation of the model

We present the PDE model for the main compartment and show how we could express it as a DDE model.

A.1. PDE model for the main compartment

From Fig. 1, we can write down a PDE satisfied by the cell density function for each compartment. We let a represents age and t time. The age-structured model for the cell populations can be written as

$$\frac{\partial m}{\partial t}+\frac{\partial m}{\partial a}=-\gamma_s(G)m \quad t>0, a\in[0,\tau_s], \tag{A.1}$$

$$\frac{\partial s}{\partial t}+\frac{\partial s}{\partial a}=-\delta(W)s-\beta(S)s, \quad t>0,\ a>0, \tag{A.2}$$

$$\frac{\partial p}{\partial t}+\frac{\partial p}{\partial a}=-\gamma_p(G)p, \quad t>0,\ a\in[0,\tau_p], \tag{A.3}$$

$$\frac{\partial n}{\partial t}+V_n(G)\frac{\partial n}{\partial a}=-\gamma_n(G)n, \quad t>0,\ a\in[0,\tau_n], \tag{A.4}$$

$$\frac{\partial w}{\partial t}+\frac{\partial w}{\partial a}=-\gamma_w w, \quad t>0,\ a>0. \tag{A.5}$$

Note that age a characterizes each compartment separately but time t is the same in all compartments. For instance, cells entering a given compartment are always characterized by $a=0$. The right hand sides of these equations account for the cell loss. To completely determine the system, we also need to provide initial conditions and boundary conditions. We consider the following boundary conditions:

$$\begin{aligned}&m(t,0)=\beta(S(t))S(t), \quad s(t,0)=2m(t,\tau_s),\\ &p(t,0)=\delta(W(t))S(t), \quad n(t,0)=A(G(t))p(t,\tau_p),\\ &w(t,0)=n(t,\tau_n),\end{aligned}$$

where $A(G)$ is the amplification factor from proliferative to non-proliferative neutrophil precursors and the total population of each type is defined as

$$\begin{aligned}&M(t)=\int_0^{\tau_s} m(t,a)\,da, \quad S(t)=\int_0^{\infty} s(t,a)\,da,\\ &P(t)=\int_0^{\tau_p} p(t,a)\,da, \quad N(t)=\int_0^{\tau_n} n(t,a)\,da,\\ &W(t)=\int_0^{\infty} w(t,a)\,da.\end{aligned}$$

Also, we use initial conditions of the form

$$\begin{aligned}&m(0,a)=\phi_m(a), \quad a\in[0,\tau_s],\\ &s(0,a)=\phi_s(a), \quad a>0,\\ &p(0,a)=\phi_p(a), \quad a\in[0,\tau_p],\\ &n(0,a)=\phi_n(a), \quad a\in[0,\tau_n],\\ &w(0,a)=\phi_w(a), \quad a>0.\end{aligned}$$

A.2. Derivation of the DDE model from the PDE model

We briefly present a generic equation for a PDE model and show how such a model can be expressed as DDEs. For a full derivation, see the review by Foley and Mackey (2009).

Let $x(t,a)$ be the cell density at time t and age a. The general form of equation for the cell density $x(t,a)$ of this model is

$$\frac{\partial x}{\partial t}+V(G(t))\frac{\partial x}{\partial a}=-\gamma(G(t))x, \quad t>0,\ a\in[0,\tau],$$

with some boundary condition $x(t,0)=H(t)$ and initial condition $x(0,a)=\phi(a)$. By integrating with respect to the age variable and using the method of characteristics to find an expression for $x(t,\tau)$ (see Webb, 1985 for more details on the method of characteristics), one obtains the following DDE:

$$\frac{dX}{dt}=V(G(t))\left[H(t)-H(t-T_\tau)\exp\left(-\int_0^{T_\tau}\gamma(G(w))\,dw\right)\right]-\gamma(G(t))X(t),$$

where $X(t)=\int_0^\tau x(t,a)\,da$ is the total number of cells at time t. Note that if the death rate γ is a constant, the equation reduces to

$$\frac{dX}{dt}=V(G(t))[H(t)-H(t-T_\tau)e^{-\gamma T_\tau}]-\gamma X(t).$$

We now apply this technique to the PDE (A.1)–(A.5) to express the model as DDE for the total population numbers $S(t), P(t), N(t)$ and $W(t)$. First, we integrate Eq. (A.2) for $s(t,a)$ with $s(t,0)=2m(t,\tau_s)$ and $\lim_{a\to\infty}s(t,a)=0$. We obtain

$$\begin{aligned}&\frac{dS}{dt}+\lim_{a\to\infty}s(t,a)-s(t,0)=-[\beta(S(t))+\delta(W(t))]S(t).\\ &\Longrightarrow \frac{dS}{dt}=2m(t,\tau_s)-[\beta(S(t))+\delta(W(t))]S(t).\end{aligned} \tag{A.6}$$

In order to get an expression for $m(t,\tau_s)$, we have to solve Eq. (A.1)

$$\frac{\partial m}{\partial t}+\frac{\partial m}{\partial a}=-\gamma_s(G(t))m, \quad t>0,\ a\in[0,\tau_s],$$

with $m(t,0)=\beta(S(t))S(t)$. We obtain

$$\begin{aligned}m(t,\tau_s)&=m(t-\tau_s,0)\exp\left(\int_0^{\tau_s}-\gamma_s(G(t))\,dt\right)\\ &=\beta(S(t-\tau_s))S(t-\tau_s)\exp\left(\int_0^{\tau_s}-\gamma_s(G(t))\,dt\right).\end{aligned}$$

Substituting $m(t,\tau_s)$ in Eq. (A.6) yields the equation for $S(t)$:

$$\frac{dS}{dt}=2\beta(S_{\tau_s})S_{\tau_s}\exp\left(\int_0^{\tau_s}-\gamma_s(G(t))\,dt\right)-[\beta(S)+\delta(W)]S. \tag{A.7}$$

Using constant apoptosis rate, the equation becomes

$$\frac{dS}{dt}=2\beta(S_{\tau_s})S_{\tau_s}e^{-\gamma_s\tau_s}-[\beta(S)+\delta(W)]S. \tag{A.8}$$

We use the notation $S_{\tau_s}:=S(t-\tau_s)$ and $G_{\tau_s}:=G(t-\tau_s)$. More generally, a subscript on a variable denotes the delay in this variable.

Next, we derive an expression for the proliferative population of precursors cells $P(t)$ by solving the PDE (A.3) with boundary condition $p(t,0)=\delta(W(t))S(t)$. Integrating with respect to a leads to

$$\frac{dP}{dt}+p(t,\tau_p)-p(t,0)=-\gamma_p(G(t))P(t). \tag{A.9}$$

The value of $p(t,\tau_p)$ is found by solving the PDE with the method of characteristics presented in Foley and Mackey (2009). We directly obtain

$$p(t,\tau_p)=\delta(W_{\tau_p})S_{\tau_p}\exp\left(-\int_0^{\tau_p}\gamma_p(G(t))\,dt\right).$$

Substituting in Eq. (A.9), we get the following DDE for the proliferative neutrophil precursors:

$$\frac{dP}{dt}=-\gamma_p(G)P+\delta(W)S-\delta(W_{\tau_p})S_{\tau_p}\exp\left(-\int_0^{\tau_p}\gamma_p(G(t))\,dt\right). \tag{A.10}$$

Similarly, we derive an equation for the non-proliferative precursors cells $N(t)$ with $n(t,0) = A(G(t))p(t,\tau_p)$ and obtain

$$\frac{dN}{dt} + V_n(G(t))[n(t,\tau_n) - n(t,0)] = -\gamma_n(G(t))N(t). \tag{A.11}$$

The value of $n(t,\tau_n)$ is given by

$$\begin{aligned} n(t,\tau_n) &= n(t-\bar{\tau_n},0) * e^{-\gamma_n \bar{\tau_n}} \\ &= A(G_{\bar{\tau_n}})\delta(W_{\tau_p})S_{\tau_p} \exp\left(-\int_0^{\tau_p}\gamma_p(G(t))\,dt - \int_0^{\bar{\tau_n}}\gamma_n(G(t))\,dt\right), \end{aligned}$$

with $\bar{\tau_n}$ satisfying

$$\tau_n = \int_{t-\bar{\tau_n}}^{t} V_n(G(w))\,dw.$$

Substituting in Eq. (A.11), we obtain a DDE for the non-proliferative neutrophil precursors:

$$\begin{aligned} \frac{dN}{dt} = &-\gamma_n(G)N + V_n(G)\delta(W_{\tau_p})S_{\tau_p}\exp\left(-\int_0^{\tau_p}\gamma_p(G(t))\,dt\right) \\ &\times\left[A(G) - A(G_{\bar{\tau_n}}) * \exp\left(-\int_0^{\bar{\tau_n}}\gamma_n(G(t))\,dt\right)\right]. \end{aligned} \tag{A.12}$$

Finally, we derive an equation for the circulation WBC population $W(t)$ by solving Eq. (A.5) with $w(t,0) = n(t,\tau_p)$ and $\lim_{a\to\infty} w(t,a) = 0$. Integrating with respect to a gives

$$\begin{aligned} &\frac{dW}{dt} + \left[\lim_{a\to\infty} w(t,a) - w(t,0)\right] = -\gamma_w W(t) \\ \Longrightarrow\ &\frac{dW}{dt} = n(t,\tau_n) - \gamma_w W(t). \end{aligned}$$

Substituting the value of $n(t,\tau_n)$ leads to the governing equation for WBCs:

$$\begin{aligned} \frac{dW}{dt} = &-\gamma_w W + A(G_{\bar{\tau_n}})\delta(W_{\tau_p})S_{\bar{\tau_p}}\exp\left(-\int_0^{\tau_p}\gamma_p(G(t))\,dt\right. \\ &\left.-\int_0^{\bar{\tau_n}}\gamma_n(G(t))\,dt\right). \end{aligned} \tag{A.13}$$

Notice that we have not derived an equation for the proliferative stem cell compartment $m(t,a)$ because it was not necessary to do so. Indeed, it can be seen from Fig. 1 that the dynamics of this compartment is included in a loop and hence, in the equation for the resting stem cells $s(t,a)$. We only solved the PDE (A.1) to get the value of $m(t,\tau_s)$ when solving for the resting stem cells $S(t)$.

Appendix B. Derivation of the fraction of bound G-CSF receptors($F(G)$)

We define an expression for the fraction $F(G)$ of G-CSF receptors that are bound. To do so, we consider more closely the process of binding of G-CSF to its receptor. On a single neutrophil, there are between 200 and 1000 binding sites. Each binding sites contain a G-CSF receptor, which can bind to two G-CSF molecules (Layton and Hall, 2006). We assume that two G-CSF molecules bind simultaneously. This could be represented by the following submodel:

$$R + 2G \underset{k_{-1}}{\overset{k_1}{\rightleftharpoons}} RG_2,$$

where R are G-CSF receptors, G is G-CSF, RG_2 is the bound complex and k_1 and k_{-1} and binding rate constants. From the law of mass action,

$$\frac{d[RG_2]}{dt} = k_1[R][G]^2 - k_{-1}[RG_2], \tag{B.1}$$

where the brackets denote concentrations. At steady state, $d[RG_2]/dt = 0$ and therefore, $k_1[R][G]^2 = k_{-1}[RG_2]$. To simplify, let us scale out one parameter and define $k = k_{-1}/k_1$. Also, let T be the total number of receptors (free and bound in the complex RG_2):

$$T = R + RG_2.$$

Thus, we obtain

$$\begin{aligned} &[R][G]^2 = k[RG_2] \\ \Longrightarrow\ &[T - RG_2][G]^2 = k[RG_2] \\ \Longrightarrow\ &[T][G]^2 = [RG_2]([G]^2 + k) \\ \Longrightarrow\ &\frac{[RG_2]}{[T]} = \frac{[G]^2}{[G]^2 + k}. \end{aligned}$$

Hence, the fraction of bound G-CSF receptors ($[RG_2]/[T]$) is given by

$$F(G) = \frac{G^2}{G^2 + k}. \tag{B.2}$$

Therefore, the expression for clearance of G-CSF is $(\gamma_G + \sigma W F(G))G$.

Appendix C. Parameter estimation

We present the parameter estimation for the main compartment as well as the G-CSF compartment (for both filgrastim and pegfilgrastim).

C.1. Parameter estimation for the main compartment

In this section, we estimate the parameters of the main part of the model using experimental data and other information from the literature. A list of the parameters is presented in Table 1. Since we are interested in studying the effects of G-CSF following chemotherapy, we need to be able to mimic the three following situations with the mathematical model:

1. *Cancer*: This set of parameters represents the characteristics of people suffering from cancer prior to chemotherapy. We do not look at a specific type of cancer, but we do consider only non-myeloid types of cancer. The parameters used for this category are the same as for healthy subjects.
2. *Chemotherapy*: The effects of myelosuppressive anti-cancer drugs are often associated with a significant incidence of severe neutropenia. We mimic chemotherapy by increasing the apoptosis rates γ_s, γ_p and γ_n (Hannun, 1997) and keeping all the other parameters fixed.
3. *G-CSF*: G-CSF is used for treating chemotherapy-induced neutropenia. The effects of G-CSF are included explicitly in the model through the functions $A(G), V_n(G), \gamma_s(G), \gamma_p(G)$ and $\gamma_n(G)$.

Age at the end of different phases τ_i: The age at the end of a given phase will not be dependent on the G-CSF concentration. To mimic the decrease or increase in the time spent in the proliferative or non-proliferative phase, we increase or decrease the aging velocity.

- τ_s: In Bernard et al. (2003), τ_s was estimated to lie between 1.4 and 4.2 days. We use the same value of 2.8 days as in Bernard et al. (2003).
- τ_p: From Israels and Israels (2002), cells spend about 6 days in the mitotic pool under normal physiological state whereas in Mackey and Dormer (1982), they estimated 3.27 days. We take $\tau_p = 5$ days.
- τ_n: The transit time through the postmitotic pool under normal physiological conditions (no exogenous G-CSF) is between 6

and 8.4 days (Israels and Israels, 2002; Price et al., 1996; Roskos et al., 2006). We take $\tau_n = 6$ days. Under G-CSF treatment, τ_n varies from 2.9 days (4.3 μg/kg) to 4.3days (0.4 μg/kg) (Price et al., 1996) and we account for this decrease by changing the aging velocity $V_n(G)$.

Aging velocities for the non-proliferative phase $V_n(G)$: We use the following bounded function for modeling the aging velocity:

$$V_n(G) = (V_{max} - 1)\frac{G}{G + b_v} + 1,$$

where V_{max} is the maximum velocity and the parameter b_v controls how fast the velocity is increasing. Notice that for $G = 0$, the velocity is 1, so that it takes τ_n days to go through the phase. We set V_{max} to τ_n, so that the minimum transit time for the postmitotic pool is one day (Lord et al., 1989). In order to determine the value of the parameter b_v, we simulated G-CSF (filgrastim and pegfilgrastim) administration in the system and fitted the model to data from Green et al. (2003) using a nonlinear least squares approach (see Fig. 10). We also ensured that the aging velocity doubles under G-CSF. Indeed, from Price et al. (1996), we have that the time spent in the postmitotic pool is reduced from 6.4 days (no G-CSF) to 2.9days (5 μg/kg G-CSF/day). Using $b_v = 0.001$ for filgrastim and $b_v = 0.08$ for pegfilgrastim, we obtain that $\bar{\tau_n}$ (time spent in postmitotic pool) ranges between 2.9 and 6 days.

Apoptosis rates γ_i: There are four apoptosis rates to consider. Three of them (γ_s, γ_p and γ_n) vary in response to G-CSF and chemotherapy, whereas we assume that the death rate from the circulating neutrophils γ_w remains unchanged during chemotherapy and G-CSF treatment. We take $\gamma_w = 2.4\,\text{days}^{-1}$ as in Bernard et al. (2003). Next, we look at the three other apoptosis rates for cancer subjects, under chemotherapy and G-CSF treatment.

- *Cancer*: To simulate non-myeloid cancer with the model, we use the same values as for healthy individuals. We take $\gamma_s = 0.07\,\text{days}^{-1}$ (Bernard et al., 2003). In Mackey et al. (2003), they estimated γ_p to vary between 0.27 and 0.31 days^{-1} (average 0.28 days^{-1}). We take $\gamma_p = 0.27\,\text{days}^{-1}$. Finally, we assume that the death rate for the proliferative and non-proliferative precursors are the same ($\gamma_n = 0.27\,\text{days}^{-1}$).
- *Chemotherapy*: It has been shown that myelosuppressive chemotherapy induces apoptosis in cells (Hannun, 1997). Moreover, it has been reported that chemotherapy can induce oscillations in the blood neutrophil count (Kennedy, 1970). Thus, we chose the death rate values so that the model displays oscillations (the minimal value so that we get oscillations). Indeed, increasing the apoptosis in the model destabilizes the system and triggers oscillations (see later). However, we need to be careful not to increase the death rates too much because it leads to failure in the system (number of proliferative cells goes below zero). Since the apoptosis rates are maximal under chemotherapy, we denote the parameters by the superscript "*max*". We take $\gamma_s^{max} = 0.2\,\text{days}^{-1}$, $\gamma_p^{max} = 0.45\,\text{days}^{-1}$ and $\gamma_n^{max} = 0.45\,\text{days}^{-1}$.
- *G-CSF*: As mentioned said above, G-CSF inhibits the chemotherapy-induced apoptosis. Therefore, we will mimic the action of G-CSF following chemotherapy by decreasing the apoptosis rates γ_S, γ_p and γ_N as a function of G-CSF. We use the following decreasing bounded functions:

$$\gamma_s(G) = (\gamma_s^{max} - \gamma_s^{min})\frac{b_s}{G + b_s} + \gamma_s^{min}, \tag{C.1}$$

$$\gamma_p(G) = (\gamma_p^{max} - \gamma_p^{min})\frac{b_p}{G + b_p} + \gamma_p^{min}, \tag{C.2}$$

$$\gamma_n(G) = (\gamma_n^{max} - \gamma_n^{min})\frac{b_n}{G + b_n} + \gamma_n^{min}, \tag{C.3}$$

where γ_i^{min} and γ_i^{max} are, respectively, the minimum and maximum values for the apoptosis rates ($i = s, p, n$) and the b_i are parameters that control the steepness of the function. We use minimum values γ_i^{min} to be the same as the cancer (healthy) values and the maximum values to be the same as the chemotherapy values. The parameters b_s, b_p and b_n have an important effect on the model's response to G-CSF administration. A low value of b_i means that the death rate will remain near its maximum value γ_i^{max} longer, whereas high values of b_i lead to a more rapid decrease toward its minimum value γ_i^{min}. Moreover, since the pharmacokinetic properties of filgrastim and pegfilgrastim are different, values differ depending on the type of G-CSF recombinant form. We used data from Green et al. (2003) to fit values (using a least squares approach as before) and obtain $b_s = 0.01$ and $b_p = b_n = 0.05$ for

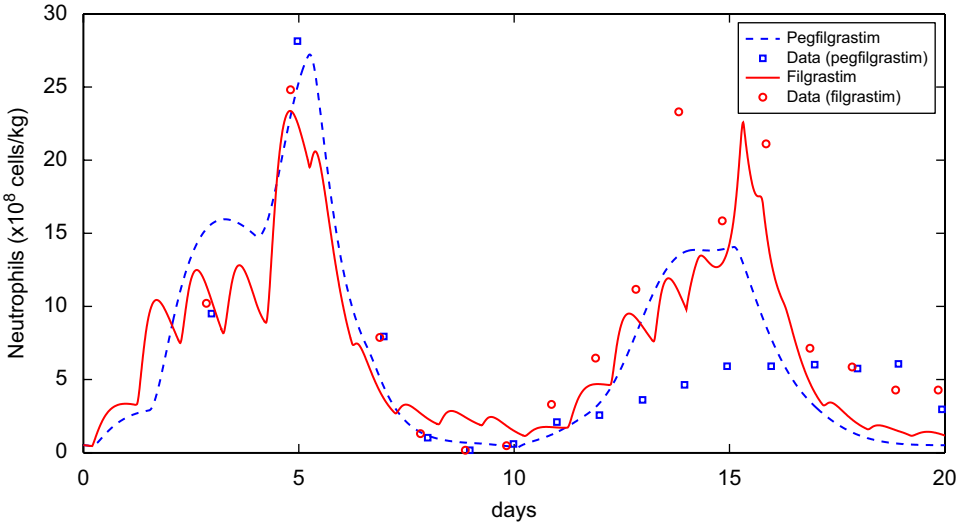

Fig. 10. Simulation of daily filgrastim (5 μg/kg) and pegfilgrastim (100 μg/kg) on cancer patients. Data (squares and circles) are taken from Green et al. (2003). Filgrastim was given for a period of 14 days. Parameters used are listed in Table 1.

filgrastim and $b_s = 0.01$ and $b_p = b_n = 1$ for pegfilgrastim (see Fig. 10).

Amplification factor $A(G)$: A study by Lord et al. (1989) reported an extra 3.2 amplification divisions in neutrophil development with added G-CSF. This corresponds to a number of effective divisions (N_E), i.e. it includes the effects of apoptosis in the mitotic compartment. However, the apoptosis rate γ_p is included explicitly in our model, and therefore we are interested in the absolute number of divisions (N_A). Using the relation $N_A = N_E e^{-\gamma_p \tau_p}$ and parameters listed in Table 1, we obtain that 3.2 effective divisions correspond to 5.1 absolute cell divisions. Roskos et al. (2006) estimated an maximum amplification factor of four extra effective divisions, corresponding to 5.8 extra cell divisions. We use a simple bounded function to model the amplification factor as a function of G:

$$A(G) = (A_{max} - A_{min})\frac{G}{G + b_A} + A_{min}. \tag{C.4}$$

In Bernard et al. (2003), they estimated that 15.2 cell divisions occur in the mitotic compartment. We use $A_{min} = 2^{16} \times 10^2$ and $A_{max} = 2^{21} \times 10^2$ so that it leads to relevant steady states values for the neutrophil number. The parameter b_A influences how fast the amplification is increased under G-CSF. The smaller b_A, the faster A increases. We simulated daily filgrastim administration (5 μg/kg) as well as a bolus 100 μg/kg of pegfilgrastim and fitted the model to data from Green et al. (2003). We obtained values of $b_A = 0.35$ (filgrastim) and $b_A = 1.05$ (pegfilgrastim) (see Fig. 10). With these values, the amplification ranges between $2^{16} \times 10^2(655)$ and $2^{18.3} \times 10^2(3700)$. For daily doses of 10 μg/kg of filgrastim, amplification goes up to approximately 4500×10^2 (18.8 divisions). This is less than the estimate of 3.2 extra effective cell divisions reported in Lord et al. (1989), but we consider this is reasonable. Lower values of b_A lead to higher ANC responses.

Differentiation rate from stem cell: $\delta(W)$ We use $\delta(W) = f_0\theta_1/(\theta_1 + W)$ as in Colijn and Mackey (2005) with $f_0 = 0.40\,\text{days}^{-1}$ and $\theta_1 = 0.36 \times 10^8$ cells/kg. This is a monotone decreasing function, accounting for the negative feedback loop in the system (if W decreases, then $\delta(W)$ increases, leading to an increase in differentiation and eventually an increase in W).

Reentry into stem cell proliferative phase $\beta(S)$: We assume that $\beta(S)$ does not depend on G-CSF and we take the decreasing Hill function $\beta(S) = k_0\theta_2^2/\theta_2^2 + S^2$ as in Colijn and Mackey (2005). Values of k_0 and θ_2 are $8.0\,\text{days}^{-1}$ and 0.3×10^6 cells/kg.

C.2. Parameter estimation for the G-CSF compartment (filgrastim)

In this section, we present the parameters used for modeling the effects of filgrastim administration with the G-CSF model presented in Fig. 2. Most of the pharmacokinetic parameters were taken from published studies on G-CSF kinetics, whereas the remaining ones were calculated or estimated using experimental data taken in the literature.

The values of the parameters are presented in Table 1. The rate constants $k_T = 0.07\,\text{h}^{-1}$ ($1.68\,\text{day}^{-1}$) and $\sigma = 0.03$ kg/h (0.72 kg/day) as well as the of the volume of blood $V_B = 76$ ml/kg are the same as in Colijn et al. (2007). The value of the endogenous production rate of G-CSF G_{prod} was taken from Vainstein et al. (2005) who estimated it as 4.83 pM/h (7.259×10^{-28} μg/(ml blood) ∗ day). To estimate the values of the constant k, γ_G and k_B, we fitted our model to the digitized data from Morstyn et al. (1989), which shows G-CSF blood levels following a bolus subcutaneous injection of 10 μg/kg (see Fig. 11) in patients who had histologically proven metastatic malignancy. We minimized the mean square error (MSE) of our model with respect to the wanted parameters using `fminsearch` in `matlab`, which implements the Nelder–Mead simplex (direct search) method for multidimensional unconstrained nonlinear minimization. Despite the fact that this method only minimizes functions locally and that our MSE function has several local minima, this method gave good results because we had good initial guesses to supply to the function. More sophisticated numerical methods that are designed for globally optimizing functions, such as simulated annealing, were tried but the results were not better while the computation time was much higher.

We estimated the value of k to be 10 and the value of γ_G to be $0.14\,\text{h}^{-1}$ ($3.36\,\text{day}^{-1}$). In Vainstein et al. (2005), they took γ_G to be $0.06\,\text{h}^{-1}$ although their value could vary between 0.01 and $0.5\,\text{h}^{-1}$. In Hayashi et al. (2001), they estimated $k_B = 0.10\,\text{h}^{-1}$ whereas

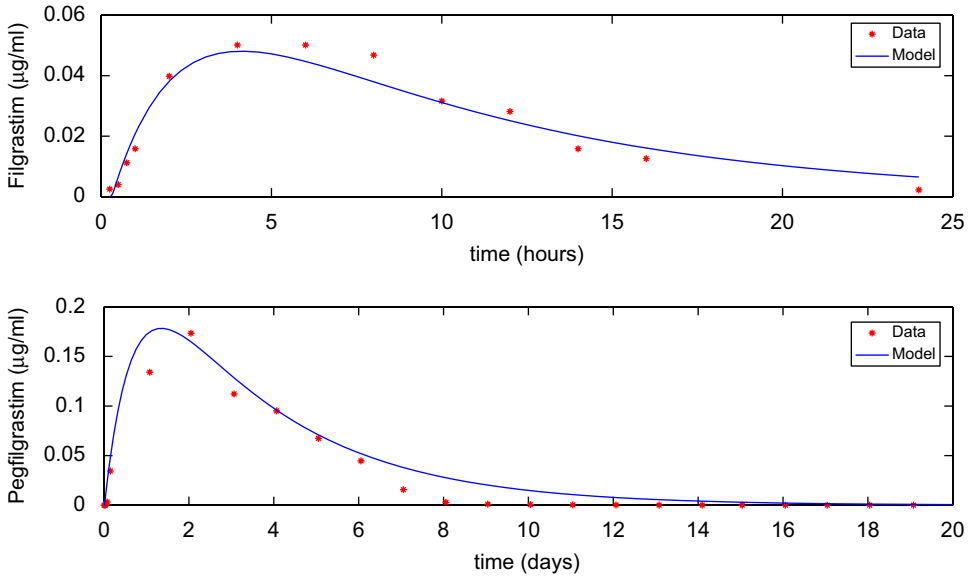

Fig. 11. Simulation of bolus subcutaneous injection using the G-CSF model (11). Top panel: filgrastim administration (10 μg/kg). The model (solid line) is compared to data from Morstyn et al. (1989) (stars). Parameters used are listed in Table 1. Bottom panel: simulation of an injection of 100 μg/kg of Pegfilgrastim using the G-CSF model (solid line). The parameters used are $N = 5.6 \times 10^8$ cells/kg, $\gamma_G = 1.4\,\text{day}^{-1}$, $k_T = 0\,\text{day}^{-1}$, $k_B = 0.32\,\text{day}^{-1}$, $\sigma = 0.01$ kg/day and $k = 0.01$. All other parameters are the same as in Table 1. Data from Zamboni (2003) are shown in red stars.

Colijn et al. (2007) used $k_B = 0.25\,\mathrm{h}^{-1}$. For our study, it was necessary to use a higher value ($k_B = 0.41\,\mathrm{h}^{-1} = 9.84\,\mathrm{day}^{-1}$) in order to reach to observed levels of G-CSF following a 10 μg/kg injection from the experimental data (Morstyn et al., 1989).

As explained above, the exogenous input function $I(t)$ was modeled by a step function. For the purpose of fitting data from Morstyn et al. (1989), we used $a = 50\,\mu\mathrm{g}/(\mathrm{kg} * \mathrm{h})$ ($a = 1200\,\mu\mathrm{g}/(\mathrm{kg} * \mathrm{day})$), $s = 0.2\,\mathrm{h}$ ($s = 0.0083\,\mathrm{d}$) and $t_{on} = 0.2\,\mathrm{h}$ ($t_{on} = 0.0083\,\mathrm{d}$), which is equivalent to a bolus injection of 10 μg/kg. Fig. 11 shows a numerical simulation of the model using parameters in Table 1.

C.3. Parameter estimation for the G-CSF compartment (pegfilgrastim)

The two-compartment model presented in Fig. 2 is used for modeling both filgrastim and pegfilgrastim administrations. However, since the pharmacokinetic properties of these two recombinant forms of G-CSF are different, some parameters need to be changed. Recall that filgrastim is cleared from the body by two mechanisms: renal clearance (the main degradation route) and neutrophil-mediated clearance (Zamboni, 2003). However, pegfilgrastim, which has a larger molecular weight, is less easily cleared by the kidneys. The predominant route of elimination for pegfilgrastim is thus by binding to neutrophil receptors. From a modeling point of view, we make the following modifications:

- Decrease the clearance parameter γ_G associated with renal clearance.
- Decrease the rates k_T and k_B between the tissue and blood compartments. Since Pegfilgrastim is a larger molecule, we assume a slower absorption into the blood (Molineux et al., 1999) and thus we decrease k_B. In their model, Roskos et al. (2006) included a time lag to account for this delayed absorption. Moreover, we assume $k_T = 0$ as in Roskos et al. (2006).
- Modify the parameter k in the function $F(G)$ (fraction of bound receptors). Recall that if we decrease the value of k, this implies that a smaller G-CSF concentration is needed for obtaining the same fraction of bound receptors.
- Modify the binding coefficient σ to account for the delayed absorption of the drug.

To estimate these parameters, we used data from Zamboni (2003) and fitted the model Eqs. (11) using the same least square approach as for filgrastim (see above). We used a constant neutrophil value of $N = 5.6 \times 10^8$ cells/kg based on ANC data reported in Zamboni (2003). We obtained the estimated values $\gamma_G = 1.4\,\mathrm{day}^{-1}$, $k_B = 0.32\,\mathrm{day}^{-1}$ and $k = 0.01$ and $\sigma = 0.01$ kg/day. Fig. 11 shows integration of the model compared to clinical data from Zamboni (2003).

Appendix D. Method for numerical simulations

We use a numerical solver for DDEs called `ddesd` (Shampine, 2005) that runs under `matlab`. For all simulations, we set the maximum time step to 0.01. Recall that the full model is given by the Eqs. (6)–(11). We first make some simplifying assumptions. The computation of $\bar{\tau_n}$ requires integrating the aging velocity over time until the area under the curve is equal to τ_n ($\tau_n = \int_0^{\bar{\tau_n}} V_n(G(w))\,dw$). It involves finding the upper bound of the integral, which depends on the shapes of $G(t)$ and $V_n(G)$ and on the value at which we start integrating (at the beginning of the phase ($a = 0$), at the current time t, etc.). For example, one could also define $\tau_n = \int_{t-\bar{\tau_n}}^{t} V_n(G(w))\,dw$. For this reason, we decided to simplify the problem and to assume that $\bar{\tau_n}$ at time t is given by $\bar{\tau_n} = \tau_n / V_n(G(t))$. This represents the instantaneous value of $\bar{\tau_n}$ and it will change as t changes. It means that if V_n was kept constant, it will take τ_n / V_n days to go through the proliferative phase. For similar reasons, we simplify the computation of $\exp(-\int_0^{\tau_s} \gamma_s(G(t))\,dt)$, $\exp(-\int_0^{\tau_p} \gamma_p(G(t))\,dt)$ and $\exp(-\int_0^{\bar{\tau_n}} \gamma_n(G(t))\,dt)$ by using, respectively, $e^{-\gamma_s \tau_s}$, $e^{-\gamma_p \tau_p}$ and $e^{-\gamma_n \bar{\tau_n}}$.

Next, we numerically integrate the mathematical model and study how the model behaves in when no G-CSF treatment is given and look at the effects of daily G-CSF (Filgrastim).

D.1. Simulation without G-CSF treatment

First, we integrate the system assuming no exogenous G-CSF is given. Since we have delayed variables, we need to specify a history function on the interval $[-\max(\tau_s, \tau_p, \tau_n), 0]$. For simplicity, we chose constant initial functions and simulated the system for several different initial values (ranging from 0 to three times the

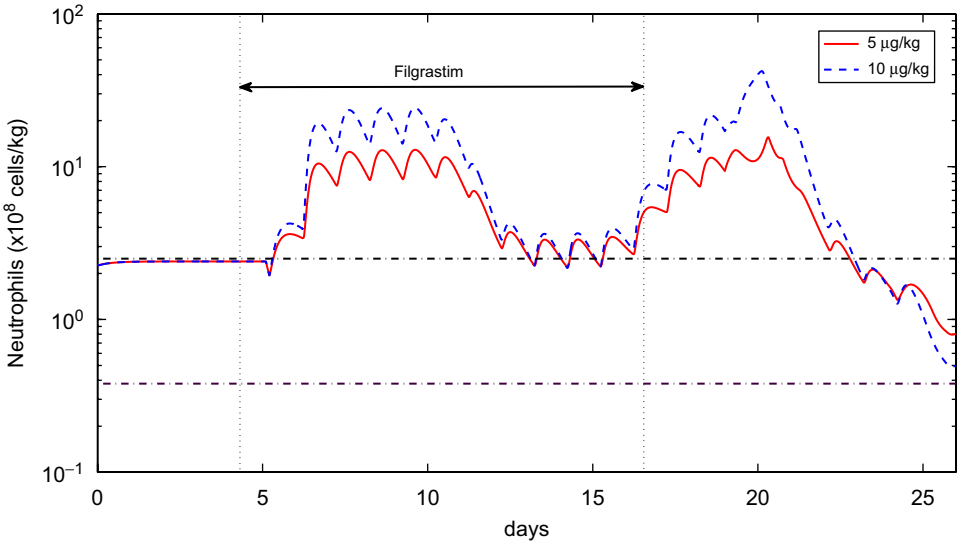

Fig. 12. Effects of varying G-CSF dose. Simulation of daily filgrastim administration in the model (before chemotherapy) during a period of 14 days for two dosages: 5 μg/kg (blue) and 10 μg/kg (red). Parameters used are listed in Table 1. The two black dotted lines indicate the level for severe neutropenia (0.38×10^8 cells/kg) and a normal neutrophils level (2.5×10^8 cells/kg).

steady state values for each state variable). We found that for these initial functions, the system settles down to a steady state after a transient of about 100 days. Let (S_*, P_*, N_*, W_*) denote the steady state solution. Using the parameters listed in Table 1, numerical simulations yield values of $S_* = 3.1 \times 10^6$ cells/kg, $P_* = 0.46 \times 10^6$ cells/kg, $N_* = 8.45 \times 10^9$ cells/kg and $W_* = 2.35 \times 10^8$ cells/kg. Values for normal subjects reported in the literature vary from one study to the another. In Bernard et al. (2003), the estimate for the stem cell numbers S_* is 1.1×10^6 cells/kg but this is an imperfect estimate for many reasons, primarily because of the lack of precision in defining and experimentally determining which cells are truly stem cells. The normal number of non-proliferative neutrophil precursors (N_*) ranges between 4.0 and 10.0×10^9 cells/kg (Vainstein et al., 2005) and is estimated at 5.59×10^9 cells/kg in Dancey et al. (1976). Finally, Bernard et al. (2003) estimated a normal blood neutrophil count W_* of 6.9×10^8 cells/kg (range between 5.0 and 10.0×10^8 cells/kg) whereas Vainstein et al. (2005) reported an average of 3.0×10^8 cells/kg (range between 2.0 and 5.0×10^8 cells/kg). Despite the apparent discrepancy for the stem cell numbers, our steady states values are similar to those reported in the literature.

We can also solve the system at steady state and get analytical expressions for the equilibrium values of S_*, P_*, N_* and W_*. See Appendix E for the analytical derivation and a proof of the uniqueness of a positive steady state.

D.2. Simulating G-CSF (filgrastim) treatment

In this section, we use our model to study the effects of daily filgrastim administration. Since we are considering only non-myeloid malignancies, we assume the same set of parameters for normal and cancer subjects. Simulations of the model for daily doses of 5 and 10 μg/kg during 14 days are shown in Fig. 12. We used constant initial functions corresponding to the steady state solutions obtained in Section D.1. One can see that neutrophils increase to 7-fold (5 μg/kg) and 17-fold (10 μg/kg) during daily G-CSF treatment, in agreement with results of Chatta and Dale (1994). The aging velocity $V_n(t)$ and the amplification factor $A(t)$ are also increased under treatment, as explained in Section C.1.

Appendix E. Analytical derivation of steady state values

In this section, we derive analytically the expressions for the steady states and show that there exists a unique positive equilibrium value. First, one needs to solve the following system of equations:

$$\left.\frac{dS}{dt}\right|_* = 0, \quad \left.\frac{dN}{dt}\right|_* = 0, \quad \left.\frac{dG}{dt}\right|_* = 0,$$
$$\left.\frac{dP}{dt}\right|_* = 0, \quad \left.\frac{dW}{dt}\right|_* = 0 \quad \left.\frac{dX}{dt}\right|_* = 0,$$

where $|_*$ denotes that the equation are evaluated at steady state values $(S_*, P_*, N_*, W_*, G_*, X_*)$. Note that at equilibrium, delayed variables remain constant (for example, $S(t-\tau_s)_* = S_*$). Assuming, $G_* = 0$ and $X_* = 0$, we first obtain expressions for the steady state values S_* and W_*:

$$\left.\frac{dS}{dt}\right|_* = 0 \implies \beta(S_*)(2e^{-\gamma_s\tau_s} - 1) = \delta(W_*) \quad (S_* \neq 0), \tag{E.1}$$

$$\left.\frac{dW}{dt}\right|_* = 0 \implies \gamma_w W_* = A_*\delta(W_*)S_* e^{-\gamma_p\tau_p - \gamma_N\tilde{\tau}_{N*}}. \tag{E.2}$$

We ignore the trivial zero solution and consider only positive solutions. Solving Eq. (E.1) for S_* in terms of W_* yields:

$$S_* = \theta_2\sqrt{\frac{k_0(2e^{-\gamma_s\tau_s} - 1)}{\delta(W_*)}} - 1. \tag{E.3}$$

Substituting into Eq. (E.2), we obtain

$$W_* = \frac{A_*\delta(W_*)}{\gamma_w}\left[\theta_2\sqrt{\frac{k_0(2e^{-\gamma_s\tau_s} - 1)}{\delta(W_*)}} - 1\right]e^{-\gamma_p\tau_p - \gamma_N\tilde{\tau}_{N*}}. \tag{E.4}$$

One can find a sufficient condition under which the system has a unique positive steady state solution (a similar proof as in Bernard et al., 2003). Let the right-hand side of the previous equation be $H(W_*)$ and $r = 2e^{-\gamma_s\tau_s} - 1$. We only need to prove that dH/dW_* is negative. Then, by the fixed point theorem, we conclude that there exists a unique positive steady state. The derivative of $H(W_*)$ with respect to W_* is

$$\frac{dH}{dW_*} = \frac{A_*\theta_2\delta'(W_*)e^{-\gamma_p\tau_p - \gamma_N\tilde{\tau}_{N*}}}{2\gamma_w}\left(\sqrt{\frac{k_0 r}{\delta(W_*)}} - 1\right) * \left(2 - \frac{1}{1 - \delta(W_*)/(k_0 r)}\right). \tag{E.5}$$

Since all parameters have positive values and $\delta'(W_*)$ is negative by definition ($\delta(W)$ is a decreasing function), we have that $H'(W_*)$ is negative if and only if the term $(2 - 1/(1 - \delta(W_*)/(k_0 r)))$ is positive. This is equivalent to showing

$$\frac{1 - 2\delta(W_*)/(k_0 r)}{1 - \delta(W_*)/(k_0 r)} > 0. \tag{E.6}$$

Sufficient conditions for this to hold are $\delta(W_*) < k_0 r/2$ and $r > 0$ ($r = 0.97$ using the parameter values in Table 1). Also, from definition of $\delta(W)$, we have that $f_0 > \delta(W)$ for all W. Therefore, a sufficient condition under which there exists one and only one positive steady state solution for W_* is

$$f_0 < \frac{k_0(2e^{-\gamma_s\tau_s} - 1)}{2}. \tag{E.7}$$

A unique solution for W_* implies a unique non-zero positive solution for S_* from Eq. (E.3). Finally, given values of S_* and W_*, one obtains values for N_* and P_* from the following relationships:

$$\left.\frac{dN}{dt}\right|_* = 0 \implies P_* = \frac{1}{\gamma_p}[\delta(W_*)S_*(1 - e^{-\gamma_p\tau_p})], \tag{E.8}$$

$$\left.\frac{dP}{dt}\right|_* = 0 \implies N_* = \frac{1}{\gamma_N}[V_{n*}\delta(W_*)S_* e^{-\gamma_p\tau_p}A_*(1 - e^{-\gamma_N\tilde{\tau}_{N*}})]. \tag{E.9}$$

Using $(X_*, G_*) = (0, 0)$ and values from Table 1 for solving Eqs. (E.3), (E.4), (E.8) and (E.9), one obtains the same steady states values as in the numerical simulations.

References

Abkowitz, J.L., Holly, R.D., Hammond, W.P., 1988. Cyclic hematopoiesis in dogs: studies of erythroid burst forming cells confirm an early stem cell defect. Exp. Hematol. 16, 941–945.

Angeli, D., Ferrell, J.E.J., Sontag, E.D., 2004. Detection of multistability, bifurcations, and hysteresis in a large class of biological positive-feedback systems. Proc. Natl. Acad. Sci. USA 101, 1822–1827.

Bagowski, C.P., Ferrell, J.E.J., 2001. Bistability in the jnk cascade. Curr. Biol. 11, 1176–1182.

Bennett, C., Weeks, J., et al., M.S., 1999. Use of hematopoietic colony-stimulating factors: comparison of the 1994 and 1997 American Society of Clinical Oncology surveys regarding ASCO clinical practice guidelines. Health Services Research Committee of the American Society of Clinical Oncology. J. Clin. Oncol. 17, 3676–3681.

Bernard, S., Belair, J., Mackey, M., 2003. Oscillations in cyclical neutropenia: new evidence based on mathematical modeling. J. Theor. Biol. 223, 283–298.

Beuter, A., Glass, L., Mackey, M., Titcombe, M., 2003. Nonlinear Dynamics in Physiology and Medicine. Springer, Berlin.

Beutler, E., Lichtman, M.A., Coller, B.S., Kipps, T., 1995. Williams Hematology. McGraw-Hill, New York.
Bhalla, U.S., Ram, P.T., Iyengar, R., 2002. MAP kinase phosphatase as a locus of flexibility in a mitogen-activated protein kinase signaling network. Science 297, 1018–1023.
Butler, R., Waites, T., Lamar, R., Hainsworth, J., Greco, F., Johnson, D., 1992. Timing of G-CSF administration during intensive chemotherapy for breast cancer (abstract). Am. Soc. Clin. Oncol. 11, 1411.
Chatta, G.S., P.T.A.R., Dale, D.C., 1994. Effects of in vivo recombinant methionyl human granulocyte colony-stimulating factor on the neutrophil response and peripheral blood colony forming cells in healthy young and elderly adult volunteers. Blood 84, 2923–2929.
Clark, O., Lyman, G., Castro, A., Clark, L., Djulbegovic, B., 2005. Colony-stimulating factors for chemotherapy-induced febrile neutropenia: a meta-analysis of randomized controlled trials. J. Clin. Oncol. 23, 4198–4214.
Colijn, C., Mackey, M., 2005. A mathematical model of hematopoiesis: II. Cyclical neutropenia. J. Theor. Biol. 237, 133–146.
Colijn, C., Foley, C., Mackey, M., 2007. G-CSF treatment of canine cyclical neutropenia: a comprehensive mathematical model. Exp. Hematol. 35, 898–907.
Cross, F.R., Archambault, V., Miller, M., Klovstad, M., 2002. Testing a mathematical model of the yeast cell cycle. Mol. Biol. Cell. 13, 52–70.
Dancey, J.T., Deubelbeiss, K.A., Harker, L.A., Finch, C.A., 1976. Neutrophil kinetics in man. J. Clin. Invest. 58, 705–715.
Drazin, P.G., 1992. Nonlinear Systems. Cambridge Texts in Applied Mathematics, University of Bristol.
Ferrell, J.E., 2002. Self-perpetuating states in signal transduction: positive feedback, double-negative feedback, and bistability. Curr. Opin. Chem. Biol. 6, 140–148.
Ferrell, J.E.J., Machleder, E., 1998. The biochemical basis of an all-or-none cell fate switch in Xenopus oocytes. Science 280, 895–898.
Foley, C., Mackey, M.C., 2009. Dynamic hematological disease: a review. J. Math. Biol. 58 (1–2), 285–322.
Foley, C., Bernard, S., Mackey, M., 2006. Cost-effective G-CSF therapy strategies for cyclical neutropenia: mathematical modelling based hypotheses. J. Theor. Biol. 238, 754–763.
Friberg, L.E., Henningsson, A., Maas, H., Nguyen, L., Karlsson, M.O., 2002. Model of chemotherapy-induced myelosuppression with parameter consistency across drugs. J. Clin. Oncol. 20, 4713–4721.
Fukuda, M., Nakato, M.A.K., 1993. Optimal timing of G-CSF administration in patients receiving chemotherapy for non-small cell lung cancer (NSCLC) (abstract). Am. Soc. Clin. Oncol. 12, 1549.
Green, M.D., Koelbl, H., Baselga, J., Galid, A., Guillem, V., Gascon, P., Siena, S., Lalisang, R.I., Samonigg, H., Clemens, M.R., Zani, V., Liang, B.C., Renwick, J., Piccart, M.J., 2003. A randomized double-blind multicenter phase III study of fixed-dose single-administration pegfilgrastim versus daily filgrastim in patients receiving myelosuppressive chemotherapy. Ann. Oncol. 14, 29–35.
Hannun, Y., 1997. Apoptosis and the dilemma of cancer chemotherapy. Blood 89, 1845–1853.
Hayashi, N., Kinoshita, H., Yukawa, E., Higuchi, S., 1999. Pharmacokinetic and pharmacodynamic analysis of subcutaneous recombinant human granulocyte colony stimulating factor (Lenograstim) administration. J. Clin. Pharmacol. 39, 583–592.
Hayashi, N., Aso, H., Higashida, M., Kinoshita, H., Ohdo, S., Yukawa, E., Higuchi, S., 2001. Estimation of RHG-CSF absorption kinetics after subcutaneous administration using a modified Wagner–Nelson method with a nonlinear elimination model. Eur. J. Pharm. Sci. 15, 151–158.
Holmes, F., O'Shaughnessy, J., Vukelja, S., Jones, S., Shogan, J., Savin, M., Glaspy, J., Moore, M., Meza, L., Wiznitzer, I., Neumann, T., Hill, L., Liang, B., 2002. Blinded, randomized, multicenter study to evaluate single administration pegfilgrastim once per cycle versus daily filgrastim as an adjunct to chemotherapy in patients with high-risk Stage II or Stage III/IV breast cancer. J. Clin. Oncol. 20, 727–731.
Israels, L.G., Israels, E.D., 2002. Mechanisms in Hematology. Core Health Services Inc.
Kearns, C.M., Wang, W.C., Stute, N., Ihle, J., Evans, W.E., 1993. Disposition of recombinant human granulocyte colony-stimulating factor in children with severe chronic neutropenia. J. Pediatr. 123 (3), 471–479.
Kennedy, B.J., 1970. Cyclic leukocyte oscillations in chronic myelogenous leukemia during hydroxyurea therapy. Blood 35, 751–760.
Koumakis, G., Vassilomanolakis, M., Barbounis, V., Hatzichristou, E., Demiri, S., Plataniotis, G., Pamouktsoglou, F., Efremidis, A., 1999. Optimal timing (preemptive versus supportive) of granulocyte colony-stimulating factor administration following high-dose cyclophosphamide. Oncology 56, 28–35.
Kuwabara, T., Kato, Y., Kobayashi, S., Suzuki, H., Sugiyama, Y., 1994. Nonlinear pharmacokinetics of a recombinant human granulocyte colony-stimulating factor derivative (nartograstim): species differences among rats, monkeys and humans. J. Pharmacol. Exp. Ther. 271 (3), 1535–1543.
Layton, J., Hall, N., 2006. The interaction of G-CSF with its receptor. Bioscience 3181–3189.
Lord, B.I., Bronchud, M.H., Owens, S., Chang, J., Howell, A., Souza, L., Dexter, T.M., 1989. The kinetics of human granulopoiesis following treatment with granulocyte colony stimulating factor in vivo. Proc. Natl. Acad. Sci., USA 86, 9499–9503.
Lotem, J., Sachs, L., 1992. Hematopoietic cytokines inhibit apoptosis induced by transforming growth factor bl and cancer chemotherapy compounds in myeloid leukemic cells. Blood 80, 1750–1757.
Mackey, M., Dormer, P., 1982. Continuous maturation of proliferating erythroid precursors. Cell and Tissues Kinetics 15, 381–392.
Mackey, M.C., 2001. Cell kinetic status of haematopoietic stem cells. Cell Prolif. 34, 71–83.
Mackey, M.C., Aprikyan, A.A.G., Dale, D.C., 2003. The rate of apoptosis in post mitotic neutrophil precursors of normal and neutropenic humans. Cell Prolif. 36, 27–34.
Meisenberg, B., Davis, T., Melaragno, A.J., Stead, R., Monroy, R., 1992. A comparison of therapeutic schedules for administering granulocyte colony-stimulating factor to nonhuman primates after high-dose chemotherapy. Blood 79, 2267–2272.
Molineux, G., Kinstler, O., Briddell, B., Hartley, C., McElroy, P., Kerzic, P., Sutherland, W., Stoney, G., Kern, B., Fletcher, F., Cohen, A., Korach, E., Ulich, T., McNiece, I., Lockbaum, P., Miller-Messana, M., Gardner, S., Hunt, T., Schwab, G., 1999. A new form of filgrastim with sustained duration in vivo and enhanced ability to mobilize PBPC in both mice and humans. Exp. Hematol. 27, 1724–1734.
Morstyn, G., Campbell, L., Lieschke, G., Layton, J.D.M., O'Connor, M., Green, M., Sheridan, W., Vincent, M., Alton, K., Souza, L., McGrath, K., Fox, R., 1989. Treatment of chemotherapy-induced neutropenia by subcutaneously administered granulocyte colony-stimulating factor with optimization of dose and duration of therapy. J. Clin. Oncol. 7, 1554–1562.
Novak, B., Tyson, J.J., 1993. Numerical analysis of a comprehensive model of M-phase control in Xenopus oocyte extracts and intact embryos. J. Cell Sci. 106, 1153–1168.
Ostby, I., Rusten, L.S., Kvalheim, G., Grottum, P., 2003. A mathematical model for reconstitution of granulopoiesis after high dose chemotherapy with autologous stem cell transplantation. J. Math. Biol. 47, 101–136.
Ozbudak, E.M., Thattai, M., Lim, H.N., Shraiman, B.I., van Oudenaarden, A., 2004. Multistability in the lactose utilization network of *Escherichia coli*. Nature 427, 737–740.
Panetta, J.C., Kirstein, M.N., Gajjar, A., Nair, G., Fouladi, M., Stewart, C.F., 2003. A mechanistic mathematical model of temozolomide myelosuppression in children with high-grade gliomas. Math. Biosci. 186, 29–41.
Perko, L., 2008. Differential Equations and Dynamical Systems. Springer, New York.
Pomerening, J.R., Sontag, E.D., Ferrell, J.E.J., 2003. Building a cell cycle oscillator: hysteresis and bistability in the activation of Cdc2. Nature Cell Biol. 5, 346–351.
Price, T.H., Chatta, G.S., Dale, D.C., 1996. Effect of recombinant granulocyte colony stimulating factor on neutrophil kinetics in normal young and elderly humans. Blood 88, 335–340.
Rahman, Z., Esparza-Guerra, L., Yap, H., Fraxchini, G., Bodey, G., Hortobagyi, G., 1997. Chemotherapy-induced neutropenia and fever in patients with metastasic breast carcinoma receiving salvage chemotherapy. Cancer 79, 1150–1157.
Roeder, I., 2006. Quantitative stem cell biology: computational studies in the hematopoietic system. Curr. Opin. Hematol. 13, 222–228.
Roskos, L., Lum, P., Lockbaum, P., Schwab, G., Yang, B.-B., 2006. Pharmacokinetic/pharmacodynamic modeling of pegfilgrastim in healthy subjects. J. Clin. Pharmacol. 46, 747–757.
Rubinow, S., Lebowitz, J., 1975. A mathematical model of neutrophil production and control in normal man. J. Math. Biol. 1, 187–225.
Santillan, M., Mackey, M.C., 2004. Influence of catabolite repression and inducer exclusion on the bistable behavior of the lac operon. Biophysics 86, 1281–1292.
Santillan, M., Mackey, M.C., Zeron, E., 2007. Origin of bistability in the lac operon. Biophys. J. 92, 3830–3842.
Scholz, M., Engel, C., Loeffler, M., 2005. Modelling human granulopoiesis under polychemotherapy with G-CSF support. J. Math. Biol. 50, 397–439.
Sha, W., Moore, J., Chen, K., Lassaletta, A.D., Yi, C., Tyson, J.J., Sible, J.C., 2003. Hysteresis drives cell-cycle transitions in Xenopus laevis egg extracts. Proc. Natl. Acad. Sci. USA 100, 975–980.
Shampine, L., 2005. Solving ODEs and DDEs with residual control. Appl. Num. Math. 52, 113–127.
Shochat, E., Stemmer, S.M., Segel, L., 2002. Human haematopoiesis in steady state and following intense perturbations. Bull. Math. Biol. 64, 861–886.
Shochat, E., Rom-Kedar, V., Segel, L., 2007. G-CSF control of neutrophil dynamics in the blood. Bull. Math. Biol. 69, 2299–2338.
Strogatz S.H., 2001. Nonlinear Dynamics and Chaos: With Applications to Physics, Biology, Chemistry and Engineering. Perseus Books Group.
Stute, N., Santana, V., Rodman, J., Schell, M., Ihle, J., Evans, W., 1992. Pharmacokinetics of subcutaneous recombinant human granulocyte colony-stimulating factor in children. Blood 79 (11), 2849–2854.
Vainstein, V., Ginosara, Y., Shohamb, M., Ranmara, D., Ianovskib, A., Agur, Z., 2005. The complex effect of granulocyte colony-stimulating factor on human granulopoiesis analyzed by a new physiologically-based mathematical model. J. Theor. Biol. 234 (3), 311–327.
Webb, G., 1985. Theory of nonlinear age-dependent population dynamics. Monographs and Textbooks in Pure and Applied Mathematics, vol. 89.
Yildirim, N., Mackey, M.C., 2003. Feedback regulation in the lactose operon: a mathematical modeling study and comparison with experimental data. Biophysics 84, 2841–2851.
Yildirim, N., Santillan, M., Horike, D., Mackey, M.C., 2004. Dynamics and bistability in a reduced model of the lac operon. Chaos 14, 279–292.
Zamboni, W., 2003. Pharmacokinetics of pegfilgrastim. Pharmacotherapy 23, 9S–14S.